Title

Role of Interleukin-23 in pulp-exposed Medication-Related Osteonecrosis of the Jaw lesions in mice

Author

Goswami, Ahana

Publication Date

2024

Peer reviewed|Thesis/dissertation

UNIVERSITY OF CALIFORNIA

Los Angeles

Role of Interleukin-23 in pulp-exposed Medication-Related Osteonecrosis of the Jaw lesions in mice

A thesis submitted in partial satisfaction
of the requirements for the degree Master of Science
in Oral Biology

by

Ahana Goswami

2024

ABSTRACT OF THE THESIS

Role of Interleukin-23 in pulp-exposed
Medication-Related Osteonecrosis of the Jaw lesions
in mice

by

Ahana Goswami

Master of Science in Oral Biology

University of California, Los Angeles, 2024

Professor Reuben Han-Kyu Kim, Chair

Introduction: Medication-related osteonecrosis of the jaw is a complication that occurs in patients who are taking anti-resorptive drugs such as bisphosphonates. We previously showed that chronic inflammation and Th17 cells are associated with MRONJ development. Differentiation of Th17 cells is highly dependent on IL-23p19, a potent proinflammatory cytokine. In this current study, we investigated the role of IL-23p19 in the pathogenesis of MRONJ using a pulp exposure-induced MRONJ mouse model.

Methodology: To examine the functional role of IL-23p19, anti-IL-23p19 antibody was administered into mice receiving high doses of Zoledronic acid. The maxillary first molars were exposed and then extracted. Mice were euthanized and maxillae, cervical lymph nodes, spleen, and blood serum were collected. MicroCT, serum ELISA, histologic evaluations, and

qRT-PCR were done to assess the protective effect of IL-23p19 neutralizing antibody on MRONJ lesions.

Results: There was a significant reduction in the number of empty lacunae and necrotic bone areas in the neutralizing IL-23p19 injection groups, without any significant reduction in the number of TRAP+ osteoclasts at the site of tooth extraction. There was also a significant reduction in the tissue localization of IL-23p19 and less differentiation of Th17 cell occurring in the cervical lymph nodes upon serum neutralization of IL-23p19.

Conclusion: Serum neutralization of IL-23p19 ameliorates pulp exposure-induced MRONJ. Our study suggests that IL-23p19 is a putative therapeutic target for treating MRONJ lesions.

The thesis of Ahana Goswami is approved.

Sotirios Tetradis

Bo Yu

Insoon Chang

Reuben Han-Kyu Kim, Committee Chair

University of California, Los Angeles

2024

TABLE OF CONTENTS

PAGES

Acknowledgments

First and foremost, I would like to express my deepest gratitude to my committee chair, **Dr. Reuben Han-Kyu Kim** for his invaluable guidance and support throughout the Master's program. His mentorship has been instrumental in my professional, educational, and career advancement.

I would like to express my sincere appreciation to my committee members **Dr. Sotirios Tetradis, Dr. Bo Yu,** and **Dr. Insoon Chang** for their guidance and time in the construction of my thesis.

I cannot thank enough **Dr. Sol Kim** and **Dr. Eun-bin Bae** for their immense guidance, teaching, and help that helped me develop the thesis. They have helped me learn new skills and shared their knowledge with me.

I would also like to thank **Dr. Wei Chen** and **Da Hae Jung** for sharing their expertise and their constant support during my Master's program.

I would like to thank UCLA and the professors who helped me in the development of my professional abilities and expanding my scientific knowledge.

Lastly, I would like to thank my family for their love and constant support and who made it possible for me to pursue a Master of Science in Oral Biology at UCLA.

Abbreviations

MRONJ/ONJ-Medication-related Osteonecrosis of the jaw/ Osteonecrosis of the jaw

IL-23- Interleukin-23

IL-23p19- p19 subunit of Interleukin 23

IL-17A- Interleukin 17A

IL-6- Interleukin 6

RORγt- Retinoic acid-related orphan receptor gamma

Foxp3- Forkhead box protein 3

IL-10- Interleukin 10

IL-1β- Interleukin 1β

TNF-α- Tumor necrosis factor alpha

IFN-γ- Interferon- γ

IL-4- Interleukin 4

IL-2- Interleukin-2

IL-8- Interleukin-8

IL-15- Interleukin-15

TGF-β- Transforming growth factor beta

Th/T_H cells- T helper cells

Th17 cells- T helper 17 cells

Treg cells-T regulatory cells

Th1/Th2 cells- T helper 1/ T helper 2 cells

JAK- Janus kinase

STAT- Signaling transducer and activator of transcription

Tyr residue-Tyrosine residue

Veh- Vehicle

Zol-Zoledronic Acid

a-IL-23p19 antibody- anti-IL-23p19 antibody/ IL-23p19 neutralizing antibody

Veh-IgG- The mice group receiving Vehicle and IgG injection biweekly

Zol-IgG- The mice group receiving Zoledronic Acid and IgG injection biweekly

Veh-a-IL-23- The mice group receiving Vehicle and IL-23p19 neutralizing antibody injection biweekly

Zol-a-IL-23- The mice group receiving Zoledronic Acid and IL-23p19 neutralizing antibody injection biweekly

1.Introduction

1.1 Medication-Related Osteonecrosis of the Jaw (MRONJ)

Medication-Related Osteonecrosis of the Jaw or MRONJ/ONJ is a detrimental oral complication of long-term bisphosphate treatment. Clinically, MRONJ is defined as an exposed area of necrotic bone without closure of the overlying mucosa or bone which can be probed through an intra or extraoral fistula(e) with incidence for at least 8 weeks. Along with that the patient should not have a history of radiation exposure to the head and neck region or should not present with metastatic bone disease (Kim, Sol *et al*., Ruggiero, Salvatore L *et al*.). Previous history of antiresorptive drugs with or without associated immunodepressants or antiangiogenic drugs must also be considered for the clinical diagnosis (Ruggiero, Salvatore L *et al*.). A recent position paper by AAOMS, 2022 considered the nonexposed bone variant as the preliminary stage of ONJ (Ruggiero, Salvatore L *et al*.).

Studies have shown that the major precipitating factor for MRONJ is dentoalveolar trauma or tooth extraction. Although extraction was found to be the leading cause, the second leading risk factor is pre-existing inflammatory dental diseases like periodontal and periapical diseases with associated periodontal surgery, dental implant placement, and endodontic surgery like apicoectomy (Marx, Robert E *et al*.). But minor trauma like intubation during general anesthesia, and trauma from impression-taking can also precipitate MRONJ development. Although iatrogenic trauma is the major cause, the presence of exostoses that is at an increased risk of trauma has also been found to be associated with it (Yazdi, Pouya Masroori, and Morten Schiodt.). Duration and the route of administration of the bisphosphonate also have a role in the development of MRONJ (Du, Wen, *et al.*). Incidence of ONJ has also been found variably associated with gender with a greater predilection for females (probably due to the use of bisphosphonates associated with underlying diseases like osteoporosis or breast cancer) or with

increased age. Also, other associated comorbidities like diabetes, cancer, or oral habits like tobacco use are also found to be variably associated with precipitation of ONJ (Ruggiero, Salvatore L *et al*.).

1.2 Association of a preexisting inflammation, IL-23, and Th17 with MRONJ precipitation

Preexisting inflammatory conditions like periapical or periodontal infection can increase the risk of development of ONJ following tooth extraction (Du, Wen, *et al*.). In our previous studies, extensive research has been done and it has been already proved that ligature-induced periodontitis can exacerbate MRONJ precipitation and further removal of the ligature before extraction of tooth reduced incidence of necrotic bone formation than compared to the groups with the ligature on, suggesting how preexisting inflammation has an indispensable role in the degree of ONJ precipitation (Williams, Drake W *et al*., Kim, Sol, *et al.*). Also, Th17 cells were found to be associated with periodontitis-associated osteonecrosis (Williams Drake W *et al.)*.

Studies have showed the association of proinflammatory IL-23 and Th17 with periapical inflammation and MRONJ precipitation. Zhang, Qunzhou, *et al*. showed that Th17 cells and elevated IL-17 cytokine levels result in the development of MRONJ along with reduced Treg and IL-10 mRNA and protein levels in jaw bone marrow. Liu, Mengyu, *et al*. showed that IL-17 is a pulpitis mediator and is promoted by increased levels of TNF-α. Hu, Y., *et al.* showed that there is an association of IL-23 with pulp and peri-radicular lesions with maximum IL-23 positive cells found on Day 35 following pulp exposure. A study by Ma, Nan *et al*. proved that apical periodontitis is induced by *P. endodontalis*-induced lipopolysaccharide-associated IL-23 expression in the periodontal cells, suggesting IL-23 has an important role in pulp-related inflammation.

Our previous study has also shown that a preexisting inflammation in the pulp and the periapical area can induce MRONJ development. Song, Minju *et al.* showed that bisphosphonate can prevent the resorption of bone at the periapical area and inhibit the development of periapical radiolucency in pulp-exposed tooth although there was increased inflammatory infiltrate and increased osteoclast infiltration at the periapical region. Along with that, pulp exposure prior to tooth extraction clearly demonstrated that periapical periodontitis led to a significant increase in necrotic bone formation and the number of osteoclasts at the site of extraction. Hadaya, Danny, *et al.* also performed an experiment with rats where they exposed the maxillary first and second molars and extracted those teeth, the result showed a similar increase in necrotic bone formation.

1.3 Cytokines, and T-cells in adaptive immunity

Study of cytokines in osteonecrosis can help in better understanding the pathological relationship between periapical inflammation and osteonecrosis. Cytokines are polypeptides secreted by leucocytes and other cells which are immunomodulators. Cytokines can be inflammatory or anti-inflammatory. Inflammatory cytokines are IL-2, IL-6, IL-8, Interferon (IFN)-γ, Tumor necrosis factor (TNF)-α. Some anti-inflammatory cytokines are IL-4 and IL-10. Cytokines are potential targets for developing therapeutic strategies against autoimmune and inflammatory diseases (Zhu, Jinfang, and William E. Paul). Cytokine production is associated with the differentiation of different subsets of the T-helper cells (T_H / Th cells).

Th cell or the naïve CD4+ T cell differentiation into specialized subsets of Th cells is important for the adaptive immune response. The type of CD4+ Th cell that is differentiated depends on the subset of the cytokines and the transcriptional factors that are activated. For example, the two important Th cell subsets that are explored in this study and the cytokines associated with them-

Th-17 cells -For many years the only known Th cell subsets were Th1 and Th2 until in 2005, Langrish, Claire L *et al*. showed that there is another subset of Th cells that are induced by the proinflammatory cytokine IL-23 and are responsible for the production of IL-17A, IL-17F, IL-6, and TNF-α and have an immense role in autoimmune inflammation that led to the discovery of the Th17 cell lineage. Th17 cells have a significant role in mediating inflammatory response, antibacterial and antifungal response and produce cytokines like IL-17A, IL-17F, IL-22, and IL-21 (Saravia, Jordy, *et al.*).

Treg cells- Treg cells have a role in autoimmune disease pathology as well as limiting chronic inflammation and inflammatory bowel disease (IBD). They have a role in maintaining homeostasis. Although IL-2 and IL-15 are suggested to have a role in Treg differentiation (Hoeppli, Romy E., *et al.*), IL-10 helps in maintaining the differentiation and function of the Treg cells (Moore KW, de Waal Malefyt R, Coffman RL, O'Garra A.).

Following cytokine stimulation, the activation of different transcriptional factors and signaling transducer and activator of transcription (STAT) family protein are important to induce specific Th-cell differentiation. For example, the essential transcriptional factor associated with the differentiation of Th17 cells is RORγt. Foxp3 is the essential transcriptional factor associated with Treg differentiation (Saravia, Jordy, *et al.*). Overall, the type of cytokine that will be produced depends on the type of antigen that is presented by the antigen-presenting cells, and the type of cytokine produced leads to the activation of transcription factors and lineage decision of Th cells. There are different other Th cell lineages like Th1, Th2 Th9, Th22, and T follicular helper (Tfh cells), some of which mediate inflammation while some are anti-inflammatory (Golubovskaya, Vita, and Lijun Wu.).

1.4 IL-23, and receptor interaction of IL-23

Il-23 is a proinflammatory cytokine belonging from the IL-12 family and is a heterodimer with an α subunit (IL-23p19) and a β subunit (IL-12p40) connected with a disulfide bond. To be biologically active, both the p40 and p19 subunits should be present in the same cell. IL-23 is produced by the activated macrophages and dendritic cells (Tang, Chunlei *et al*., Pastor-Fernández, Gloria *et al*.).

IL-23 binds to IL-23R and the IL-12Rβ1, but not with IL-12β2. The IL-23R is expressed by the NK cells, monocytes/ macrophages, dendritic cells, and the activated memory T cells, but not on naive T cells. On the other hand, IL-12β1 is expressed by the T cells, NK cells, and the dendritic cells. The IL-23p19 subunit binds to the IL-23R chain and the p40 subunit interacts with the IL-12Rβ1 chain (Pastor-Fernández, Gloria *et al*., Boniface, Katia, *et al*.).

Both subunits of IL-23 interact with the receptors and activates the JAK family of tyrosine kinase and oligomerization of the receptor induces membrane conformational changes and brings JAKs to close proximity. JAK activation causes phosphorylation of the Tyr residues at the cytoplasmic end of the receptors and activated JAKs phosphorylates STAT, specifically STAT3 which dimerizes and translocate into the nucleus, binds to DNA, and leads to target gene activation (Pastor-Fernández, Gloria, *et al*.).

1.5 Rationale, Hypothesis, and Aims

The current ongoing study in our lab by Bae, Eun-bin *et al.* showed a significantly reduced number of empty lacunae and percentage of necrotic bone area at the site of the extraction socket when IL-23p19 neutralizing antibody was injected in mice along with Zoledronic acid administration when periodontitis was induced by placing ligatures in the 2nd molars in mice. However, in ligature-induced periodontitis, factors like associated constant physical trauma from the ligature silk and bacteria on the periodontal silk might change the

periodontal microenvironment and housing of different variety of immune cells. In the pulp exposure model, pulpal and periapical inflammation is solely microbial and there is no incidence of constant physical insult. Moreover, inflammation is exclusively enclosed within the alveolar bone area which might help in better understanding of the immune-mediated MRONJ pathogenesis.

In our previous study performed by Song, Minju *et al.* the experimental mice were injected with 125 μg/kg of Zoledronic Acid and the control mice were injected with 0.9% of NaCl solution. One week after the start of injection, pulp was exposed in the maxillary first molars and three weeks following the pulp exposure, the first molars were extracted. After allowing a healing period of three weeks, mice were euthanized and maxillae were collected. The necrotic bone formation and infiltration of inflammatory cells around necrotic bone area was found to be significantly high when the pulp was exposed before tooth extraction in mice treated with Zoledronic acid. We performed immunofluorescence staining on these samples in the tooth extraction sockets for IL-23p19 antibody and the results showed a significantly high number of IL-23+ cells in the area of intense inflammatory cell infiltration around the necrotic bone area when the pulp was exposed before tooth extraction compared to when only tooth was extracted and mice were treated with Zoledronic acid (Figures 1A-B). This suggests that IL-23p19 is highly expressed in the necrotic bone area in pulp-exposed MRONJ lesions in mice.

Hence in the present study, we hypothesize that IL-23p19 plays an important role in the precipitation of MRONJ lesions and targeting or blocking IL-23p19 can rescue MRONJ lesion development. The first aim for this study is to determine if IL-23p19 neutralizing antibody can ameliorate pulp exposure-induced MRONJ lesions in mice. The next aim is to determine the local (in cervical lymph node) and systemic (spleen and serum) inflammation status of IL-23/Th17 axis in mice treated with IL-23p19 neutralizing antibody. We performed MicroCT and ELISA to validate the effect of Zoledronic acid and IL-23p19 neutralization antibody. For the

first aim, we performed histological analysis to assess the number of empty lacunae, and the percentage of necrotic bone area and TRAP staining to determine any changes in the osteoclast number at the tooth-extraction site following pulp exposure. As part of the secondary aim, this study seeks to investigate tissue localization(local) of IL-23p19 and T cells that occurs upon IL-23p19 neutralization in pulp exposure-induced MRONJ model. For that, Immunofluorescence staining was performed to assess the levels of IL-23p19 cytokine and IL-23R in the necrotic bone area to assess localization of the cytokines and the T cells around the necrotic bone. The changes in the mRNA levels of different proinflammatory cytokines and transcription factors in cervical lymph node (local) and spleen (systemic) was done to estimate T-cell lineage decisions. To test that quantitative real-time PCR (qRT-PCR) of cervical lymph nodes and spleen were done for cytokines and transcription factors. The serum (systemic) proinflammatory cytokine levels were also assessed when IL-23p19 was neutralized in pulp exposure-induced MRONJ lesions using Enzyme-linked Immunosorbent Assay (ELISA).

2.Materials and Methods

2.1 Animals used

5-week-old C57/BL6J mice were purchased from The Jackson Laboratory and were kept in a pathogen-free condition under the Division of Laboratory Medicine (DLAM), University of California, Los Angeles. Throughout the experimental timeline, the mice were housed in a standard cage (4 mice/cage), maintaining a 12-hour light-dark cycle. They were given a standard diet and water ad libitum. The experimental protocols were approved by the Animal Research Committee (Protocol #: R-22-012) and were conducted according to the guidelines of the UCLA Institutional Animal Care and Use Committee (IACUC).

2.2 Drugs used

0.9% NaCl was purchased from the DLAM Pharmacy while the Zoledronic acid used was obtained from Accord (NDC 16729-242-31, 4 mg/5 mL). InVivoMAb rat IgG1 isotype control, anti-horseradish peroxide (Catalog # BE0088), InVivoMAb anti-mouse IL-23 (p19) (Clone G23-8; Catalog # BE0313), and InVivoPure pH 7.0 Dilution Buffer (Catalog # 1P0070) were obtained from BioXCell (New Hampshire 03766, USA).

2.3 Mouse model

The animals were kept in quarantine for 1 week after which they were divided into 4 groups (5 mice/ group). In order to induce osteonecrosis of the jaw, a high dose of Zoledronic acid was injected in the mice. The Zoledronic acid-IgG (Zol-IgG) and the Zoledronic acid-anti-IL-23 antibody (Zol-a-IL-23) groups received 100 µL of Zoledronic acid diluted in 0.9% NaCl at a dose of 200 µg/Kg (de Molon, Rafael Scaf, *et al.*) and the control groups i.e. the Vehicle-IgG (Veh-IgG) and the Vehicle-anti-IL-23 antibody (Veh-a-IL-23) groups were injected with 100 µL of 0.9% NaCl. All injections were done twice weekly (Mondays and Thursdays). The Veh-IgG and the Zol-IgG group received 50 µg/Kg of InVivoMAb rat IgG1 isotype control, anti-horseradish peroxide injection diluted in InVivoPure pH 7.0 Dilution Buffer while the Veh-a-IL-23 and the Zol-a-IL-23 groups were injected with InVivoMAb anti-mouse IL-23 (p19) diluted in InVivoPure pH 7.0 Dilution Buffer at a dose of 50 µg/Kg, biweekly (Tuesdays and Fridays) (Coffelt, Seth B *et al.*). All injections were done intraperitoneally. One week following the start of injections, the maxillary first molars on both sides were exposed using a ¼ round bur on a high-speed contra-angle handpiece attached to a portable dental unit and explored using No. 15 K-file. The exposed teeth were left open to the oral environment without any dressings. 5 weeks following the exposure of the molars, the same teeth were atraumatically extracted. The time point of tooth extraction was decided based on the study by Hu, Y., *et al.*, where they showed that there is an association of IL-23 with pulp and peri-radicular lesions in pulp exposure model with maximum IL-23 positive cells found on Day 35 following pulp

exposure. Hence, we decided to perform tooth extraction at 5 weeks following pulp exposure to assess the optimum role of the IL-23p19 on the development of osteonecrosis of the jaw. The pulp exposure and the tooth extractions were done under full anesthesia with a Ketamine/Xylazine cocktail in the ratio of 7:1 diluted in 0.9% NaCl. A non-steroidal anti-inflammatory drug Carprofen (Rimadyl, 50mg/mL) was diluted in 0.9% NaCl and administered subcutaneously at the dose of 5mg/Kg post-procedure for the purpose of pain relief. After allowing a healing period of 10 days, all mice were sacrificed with isoflurane overdose and cervical dislocation. This time point was also decided based on the immunofluorescence data procured from Song, Minju *et al.*'s samples where sacrifice was performed 3 weeks following the time of extraction. Although the IL-23 positive cells were found to be significantly high in the Zoledronic acid treatment group where the pulp was exposed before tooth extraction, we believed the assessment of the role of IL-23 or other cytokines would be best right after primary healing is complete (Figure 2).

2.4 Tissue procurement

Following euthanasia, mice maxillae, cervical lymph nodes, spleen, and blood serum were procured. The maxillae were kept overnight in 20 mL of 4% paraformaldehyde in 10x PBS, pH 7.4 at 4º C for fixation of the tissues. The tissues were washed with 1x PBS (3 times, 5 minutes in rocker/wash) and distilled water (3 times, 5 minutes in rocker/wash) and were shifted into 70% ethanol for tissue storage. The blood samples collected were allowed to thaw for 20 minutes and were centrifuged at 8000 rpm for 15 minutes. The serum supernatant was transferred to a 1.5 mL Eppendorf tube and stored at -80º C. The lymph nodes were crushed in the Lysis Buffer provided in the PureLink^{TM} RNA Mini Kit (Catalog number: 12183018A, Invitrogen, Carlsbad, CA, USA) with 2-mercaptoethanol and stored at -80º C.

2.5 MicroCT (µCT) scanning

The maxillae were wrapped in 70% ethanol-soaked gauze and were secured in a 15 mL conical tube for μCT scanning. The tissues were scanned using the SkyScan 1275 (Bruker Micro-CT, Kontich, Belgium) using parameters of 1.0 mm aluminium filter at 60 kVp and 166 μA, using a cylindrical tube. Reconstruction of the scanned sections were done using the NRecon software and the two-dimensional (sagittal and coronal sections) and three-dimensional images were constructed using the CTAn and CTvol software respectively (Bruker microCT, Kontich, Belgium). Bone volume (BV; mm^3) and tissue volume (TV, mm^3) were measured using the CTAn software, and the percentage bone volume over tissue volume (BV/TV) was calculated.

2.6 Decalcification

Following μCT scanning, the maxillae that were stored in 70% ethanol were washed again with 1x PBS (3 times, 5 minutes in rocker/wash) and distilled water (3 times, 5 minutes in rocker/wash) and were transferred in 20 mL of decalcification buffer made with 7% Ethylenediaminetetraacetic acid (EDTA) (EDTA disodium salt dihydrate for biotechnology, VWR Life Science, Catalog number: 97061-018) in distilled water, pH 7.4-7.6, 4º C to allow tissue decalcification. The decalcification buffer was changed every day and the tissues were placed in a rocker at 4º C for a total period of 4 weeks.

2.7 Tissue embedding and preparation

At the end of 4 weeks, the maxillae were washed again with 1x PBS (3 times, 5 minutes in rocker/wash) and distilled water (3 times, 5 minutes in rocker/wash) and were transferred in 70% ethanol. The tissues were then submitted to the Translational Procurement Core Laboratory (TPCL), University of California, Los Angeles for paraffin embedding. The maxillae were trimmed by making sagittal cuts at the distal end of the third molar and the mesial end of the first molars and finally embedded in paraffin. 5μm Formalin-Fixed Paraffin-

Embedded (FFPE) tissue sections were obtained using the microtome perpendicular to the long axis of the alveolar ridge along the distal root of the first molar extracted socket. The sections were mounted to the Fisherbrand™ Superfrost™ Plus Microscope Slides (Catalog number: 12-55-15). The specific region of interest (extraction socket of the maxillary first molars) was identified by checking the sections under the compound light microscope.

2.8 Enzyme-linked Immunosorbent assay (ELISA)

The serum samples were thawed out from -80º C and the serum levels of IL-23p19, IL-17A, IL-17F, and IL-12 were detected by sandwich ELISA technique using Mouse IL-23 Quantikine ELISA kit (R &D Systems, Catalog #: M2300), Mouse IL-17A ELISA Kit-Quantikine (R & D Systems, Catalog #: M1700-1), Mouse IL-17F ELISA Kit- Quantikine (R & D Systems, Catalog #: M17F0), and Mouse IL-12 p70 (R & D Systems, Catalog #: M1270-1) kits respectively. All the procedures were performed according to the manufacturer's protocols. The color reaction was stopped using the Stop solution (provided in the kit) as per the protocol and absorbance was read immediately at 450nm using a microplate reader (Synergy H1 microplate reader and BioTek Gen5™ All-In-One Microplate Reader Software version 2.03.1). The absorbance values of the standard were compared with the concentrations of the standard and a standard curve was plotted. The cytokine concentrations were calculated using the standard curve obtained and plotted in pg/mL.

2.9 Histomorphometric Analysis

5 sections were selected at regular intervals (every 6th slide) and were stained with hematoxylin and eosin (H and E) in order to identify and quantify the number of empty lacunae and necrotic bone areas. The sections were deparaffinized at 60º C for 1 hour and were serially rehydrated in xylene (2 times, 5 minutes each) and decreasing concentrations of ethanol (100%- 2 times, 1 minute each, 95%- 2 times, 1 minute each, 70%- once for 1 minute) and finally

washed in tap water (2 times, 1 minute each). The sections were then stained with Hematoxylin 1 (Epredia™ 7221) for 2.5 minutes and washed in running tap water until the extra stain was washed out properly. The samples were washed again in 95% ethanol for 1 minute and then stained with Eosin Y (Epredia™ 7111) for 45 seconds. The stained sections were washed in running tap water as long as all the stains were washed out properly. The samples were then serially dehydrated in increasing concentrations of ethanol (70% ethanol- once for 1 minute, 95% ethanol- 2 times, 1 minute each, 100% ethanol- 3 times, 1 minute each) and xylene (3 times, 5 minutes each) and finally mounted using Cytoseal™ 60 (Epredia™ Cytoseal™ Mountant, VWR Catalog Number: 48212-187). The samples were allowed to dry for 24 hours followed by digital imaging of the region of interest was done under an Olympus microscope (model BX51, Olympus, Tokyo, Japan) at 100x magnification showing the extracted first molar socket starting from the buccal plate to the palatal suture horizontally and the tip of the socket to the base of the palate vertically. The empty lacunae were counted and the necrotic bone area was identified as the area with 5 or more empty lacunae. The total and the necrotic bone area were measured using the ImageJ software v1.54g (NIH, Bethesda, MD). Empty lacunae were quantified as the number of empty lacunae per mm^2 total bone area. The percentage of necrotic bone area was quantified as the area with 5 or more empty lacunae/ mm^2 total bone area.

2.10 Tartrate-resistant Acid Phosphatase (TRAP) staining

4 sections were selected (every slide next to the H and E-stained section) from each sample and were deparaffinized at 60ºC for 1 hour. The slides were serially rehydrated in xylene (2 times, 5 minutes each) and in decreasing concentrations of ethanol (100%- 2 times, 1 minute each, 95%- 2 times, 1 minute each, 70%- once for 1 minute). The samples were then washed in the running tap water (2 times, 1 minute each) and were stained using the Leukocyte Acid Phosphatase (TRAP) Kit (Sigma-Aldrich, Ref: 387A-1KT). 200 µL of the TRAP staining

solution (prepared from the reagents provided in the kit) was added per slide. The slides were placed in a humidification chamber (HybEZ Oven) and incubated in the dark at 37º C for 30 minutes. The staining was checked periodically and at the end of 30 minutes, the slides were washed in running tap water to prevent any overstaining incident. The samples were then counterstained with 0.02% Fast Green in distilled water for 8 minutes, after which they were washed thoroughly and left in the chemical fume hood until they were completely air-dried. Finally, the slides were dipped momentarily in Xylene and mounted using the Cytoseal™ 60 (Epredia™ Cytoseal™ Mountant, VWR Catalog Number: 48212-187). After 24 hours of air-drying, the samples were digitally imaged under the Olympus microscope (model BX51, Olympus, Tokyo, Japan) at 100x magnification. The osteoclasts were identified as large, multinucleated cells with deep magenta-stained nuclei and were quantified as the number of osteoclasts per mm^2 of total bone area. The total bone area was quantified using the ImageJ software v1.54g (NIH, Bethesda, MD).

2.11 Immunofluorescence staining

Immunofluorescence staining was performed for IL-23p19 and IL-23R. One representative section from each sample was chosen after comparison with the H and E-stained images and the sections were incubated overnight at 60º C. The samples were serially rehydrated in Xylene (2 times, 5 minutes each) and in decreasing concentrations of ethanol (100%- 2 times, 2 minutes each, 95%- 2 times, 2 minutes each, 70%- once for 2 minutes). Antigen was retrieved by immersing the samples in diluted Antigen Unmasking Solution, citrate-based (Vector Laboratories, H-3300) at 97º C for 30 minutes after which the samples in the antigen-retrieval solution were allowed to cool down to 25º C. The sections were then washed in distilled water (3 times, 5 minutes each wash) and 1x PBS (once for 5 minutes). The samples were then rimmed using an ImmEdge Pen and were permeabilized in a solution of 0.1% Tween-20 in 1x PBS for 5 minutes. The antigen was blocked using 3% goat serum diluted in a

solution with Animal-Free Blocker, 5x concentrate (Vector Laboratories, SP-5030-250), 10% Tween-20, 20% SDS in distilled water for 1 hour. The primary antibody (Mouse IL-23p19 Polyclonal Goat IgG, Catalog #: AF 1619, biotechne, R & D Systems or Rabbit polyclonal antibody to IL-23R, Catalog number AB175072, Abcam) was diluted in the same diluent used to dilute goat serum (Ratio 1:100). 190 µL of it was applied to each sample and incubated overnight in a moist environment. The samples were then washed in 0.1% Tween-20 in 1x PBS (3 times, 5 minutes each). A secondary antibody conjugated with Alexa Flour™ 594 goat anti-rabbit IgG (H+L) (Invitrogen, Catalog # A-11012) or Alexa Flour™ 568 donkey anti-goat IgG (H+L) (Invitrogen, Catalog # A-11057) was used respectively, diluted in the same diluent as the primary antibody (Ratio 1:250) and was applied to each section (190µL). After 1 hour of incubation in dark, the samples were washed in 0.1% Tween-20 in 1x PBS (3 times, 5 minutes each) and then mounted with DAPI containing mounting medium (Vectashield Vibrance Antifade Mounting Medium with DAPI, Catalog number- H-1800). After 24 hours of drying, the samples were imaged using an Olympus Fluoview confocal microscope (model FV10i) at magnifications of 30x and 60x. The samples were quantified by counting the number of positive signals around the necrotic bone area per mm^2 of total bone area at 30x magnification. The total bone area was quantified using the ImageJ software v1.54g (NIH, Bethesda, MD).

2.12 RNA isolation and quantitative Real-time Polymerase Chain Reaction (qRT-PCR)

Total RNA was isolated from the cervical lymph node and spleen samples using the PureLink™ RNA Mini Kit (Catalog number: 12183018A, Invitrogen, Carlsbad, CA, USA) according to the manufacturer's protocol. The concentration and quality of the isolated mRNA were assessed using the NanoDrop Spectrophotometer (model ND-1000, ThermoFisher Scientific). Complementary DNA or cDNA was synthesized using the SuperScript II FirstStrand Synthesis system, Reverse Transcriptase (Catalog number: 18064014, Invitrogen), and Random Primers (Catalog number: 48190011, Invitrogen) using SimpliAmp Thermal

Cycler (Applied Biosystems by life technologies). 20 µL cDNA obtained was diluted in 80 µL UltraPure™ DNase/RNase-Free Distilled Water (Invitrogen). 2 µl of the diluted cDNA was loaded in MicroAmp Optical 96-well Reaction plate (Applied Biosystems by life technologies, Catalog number: N8010560) and was amplified in PowerUp™ SYBR™ Green Master Mix (Applied Biosystems™, Catalog number: A25742) using the QuantStudio^{TM} 3 Real-Time PCR system (Applied Biosystems by life technologies, Catalog number: A28567) using primers for *mGAPDH*, *IL-23p19*, *IL-17A*, *RORγt*, *IL-6*, *Foxp3*, *IL-10*, *IL-1β* and, *TNF-α* primers. The data was analyzed using the QuantStudio 3/5 Real-Time PCR software. The second derivative of the Cq/ Ct values of the genes were compared with the *mGAPDH* values and fold changes for the genes were assessed ($2^{-\Delta\Delta Ct}$) using the comparative ΔCt method.

2.13 Statistical analysis

All statistical analyses were done using GraphPad Prism 10.2.1 software. The outcome measurements were expressed as the mean ± standard deviation. One-way analysis of variance with Tukey's post hoc test was used to compare the outcome between the 4 groups. The data was considered statistically significant with a value of $p < 0.05$.

3.Results

3.1 Validation of Zoledronic Acid treatment

To investigate the effects of treatment with Zoledronic Acid in conjunction with the neutralization antibody, we performed µCT analysis of the extraction socket. As expected, Zoledronic acid treatment group showed reduced incidence of roughened borders of the extraction socket and unfilled tooth socket in both the Zol-IgG and Zol-a-IL-23 groups, suggesting that Zoledronic Acid has worked well in this model even in the presence of the neutralizing antibody (Figure 3).

3.2 Validation of IL-23p19 neutralizing antibody treatment

The next step was to validate the injection of IL-23p19 neutralizing antibody. The neutralization of IL-23p19 cytokine was confirmed by performing the ELISA for IL-23p19 which showed that the serum concentration of IL-23p19 was at an undetectable level (****$p<$ 0.0001) in the groups that received the IL-23p19 neutralizing antibody injection (Figure 4), suggesting IL-23p19 has also worked well in this model.

3.3 IL-23p19 neutralizing antibody ameliorates pulp-exposed MRONJ lesions in mice

To examine if neutralizing IL-23p19 can prevent the precipitation of MRONJ lesions, maxillary tissue sections were stained with H and E and then empty lacunae were counted and the percentage of necrotic bone area was evaluated. The Zol-IgG group was found to have a marked increase in the number of empty lacunae (****$p < 0.0001$) and necrotic bone (***$p <$ 0.001) upon pulp exposure, which is consistent with our previous study (Song, Minju, *et al*.). As a result of IL-23p19 neutralization, there was a significant reduction in the number of empty lacunae (**$p < 0.01$) and necrotic bone percentage (**$p < 0.01$) in the Zol-treated group, the number and percentage being consistent with that of the Veh-IgG and the Veh-a-IL-23 group. Moreover, the percentage of necrotic bone formed in the Zol group on treatment with neutralizing antibodies was almost half of that of the Zol-IgG group. This data clearly suggests that IL-23p19 has a pathogenic role in the development of MRONJ lesions and neutralizing IL-23p19 can result in the prevention of MRONJ development (Figures 5A-C).

3.4 IL-23p19 neutralizing antibody does not affect osteoclast recruitment at the MRONJ lesion sites

To examine if IL-23p19 neutralization has any role in recruiting the osteoclasts at the site of necrotic bone formation, tissue sections were stained for TRAP and the number of TRAP+ osteoclasts were counted. There was no significant change in the number of osteoclasts

between the Veh-IgG and the Zol-IgG group. Along with that, there was also no significant difference in the number of TRAP+ osteoclasts when neutralizing IL-23p19 antibody was injected in the Zol-treated group compared to the Zol-IgG group, indicating that neutralizing IL-23p19 does not have any effect on the recruitment of osteoclasts at the necrotic bone areas of MRONJ lesions (Figures 6A-B).

3.5 Serum neutralization of IL-23p19 leads to reduced IL-23p19 expression in the osteo-mucosal tissues

To assess the localization of IL-23p19 cytokine in the extraction socket area, Immunofluorescence staining was done for IL-23p19, and sections were then observed using a confocal microscope. The result showed a significant increase (**$p< 0.01$) in the levels of IL-23p19+ cells around the necrotic bone in the pulp-exposure model on Zoledronic Acid administration which is consistent with the Immunofluorescence data obtained from Song, Minju *et al.*'s samples. Moreover, there was a significant decrease in the levels of IL-23p19+ cells around the necrotic bone in the Zol-treated and Veh-treated groups upon serum IL-23p19 neutralization, indicating tissue localization of IL-23p19 is pathogenic for the development of MRONJ lesions and serum neutralization of IL-23p19 leads to reduced tissue localization of IL-23p19 (Figures 7A-B).

3.6 Serum neutralization of IL-23p19 leads to unaltered expression of IL-23R in tissue

To assess the change in the localization of T cells, we performed Immunofluorescence staining for IL-23R. The result did not show any significant difference in the IL-23R+ cells in between groups, which indicate that upon neutralization of IL-23p19, there is no alteration in the expression of IL-23R+ cells in the necrotic bone area (Figures 8A-B).

3.7 IL-23p19 neutralizing antibody causes reduced IL-23p19 synthesis in the cervical lymph nodes and reduced pathogenic Th17 cell differentiation

To further detect the effect of neutralizing IL-23p19 cytokine in serum on the cervical lymph nodes and differentiation of Th17 cells, RT-PCR was performed to obtain the mRNA expression levels for *IL-23*, *IL-17A*, *RORγt*, and *IL-6* to understand the Th17 cell lineage differentiation in the cervical lymph nodes. RT-PCR for *IL-1β* and *TNF-α* was performed to check the overall inflammation burden. *IL-23p19* mRNA expression level was found to be significantly high on administration of Zol-IgG compared to the group that received Veh-IgG when pulp was exposed prior to tooth extraction (*$p< 0.05$). However, upon neutralization of serum IL-23p19, the mRNA level of *IL-23p19* in cervical lymph nodes was found to be significantly decreased in both Zol (***$p< 0.001$) and Veh-treated groups (**$p< 0.01$) compared to the Zol-IgG group, and the level of *IL-23p19* mRNA levels in these two groups was similar to the Veh-IgG group. Interestingly, there was no significant difference in the mRNA levels of *IL-17A* between the groups. Moreover, the *RORγt* mRNA level was found to be significantly increased (*$p< 0.05$) in the Zol-a-IL-23 group compared to the group that received Zol-IgG. Similarly, for *IL-6*, mRNA level was found to be significantly increased (*$p< 0.05$) in the Zol-a-IL-23 group compared to the Zol-IgG group, suggesting that some levels of differentiation of Th17 cells might be taking place in the cervical lymph nodes, even upon serum neutralization of IL-23p19 (Figures 9A).

To confirm the phenotype of the Th17 cell, we performed the RT-PCR to check the m levels of *IL-1β* and *TNF-α*. Although there was no significant difference in the mRNA levels of *TNF-α*, *IL-1β* mRNA level was significantly reduced (*$p< 0.05$) upon neutralization of IL-23p19 in the Zol-treated group, suggesting a decrease in the inflammation burden and less differentiation of pathogenic Th17 cells (Figure 9B).

3.8 IL-23p19 neutralization causes increased Treg differentiation in the draining cervical lymph nodes

Further, RT-PCR for *Foxp3* and *IL-10* was performed to assess the Treg cell differentiation. The result showed a significant increase (*$p< 0.05$) in the mRNA levels of *Foxp3* and *IL-10* in the Zol-a-IL-23 group compared to the Zol-IgG group, which suggest differentiation of more Treg cells occurring upon serum neutralization of IL-23p19 (Figure 10).

3.9 IL-23p19 neutralizing antibody leads to reduced inflammatory cytokine levels in serum

To examine if a-IL-23p19 antibody suppresses other pathogenic cytokines like IL-17A. IL-17F and IL-12 systemically, we collected blood samples from the mice and measured the serum concentrations of IL-17A, IL-17F, and IL-12 cytokine levels. The neutralization of IL-23p19 cytokine was already confirmed by performing the ELISA for IL-23p19 which showed that the serum concentration of IL-23p19 was at an undetectable level (****$p< 0.0001$) in the groups that received the IL-23p19 neutralizing antibody injection. To further check the IL-17A. IL-17F, and IL-12 serum levels upon IL-23p19 neutralization, we performed ELISA for these three pathogenic cytokines. The results showed undetectable levels of IL-17A (****$p< 0.0001$) and IL-17F (****$p< 0.0001$) cytokine levels upon neutralization of IL-23p19, which indicated the role of IL-23p19 in the production of the pathogenic cytokines by Th17 cells and neutralization of IL-23p19 leads to depletion of serum levels of IL-17A and IL-17F (Figures 11A-B). The data also suggest that IL-23p19 is upstream and it is clear that it has an important role in the differentiation of the Th17 cells. Moreover, upon administration of IL-23p19 neutralizing antibody, serum IL-12p70, another proinflammatory cytokine was significantly reduced (*$p< 0.05$) (Figure 11C). All these data suggest that IL-23p19 neutralization in serum leads to reduced serum levels of other inflammatory cytokines. Moreover, there was no significant difference in the levels of all these cytokines in between the Veh-IgG and Zol-IgG groups, suggesting that Zol itself does not change the levels of these pathogenic cytokines in serum.

3.10 IL-23p19 neutralizing antibody has no effect on IL-23p19 and pathogenic Th17 cell differentiation in spleen

To further assess the systemic effect of IL-23p19 neutralization, we performed the qRT-PCR in the spleen samples for *IL-23p19*, *IL-17A*, *ROR-γt*, and *IL-6* primers. The result showed no significant difference of the mRNA levels in between the groups, even when IL-23p19 was neutralized (Figure 12). The result indicates that IL23p19 neutralization in serum does not have any effect on the differentiation of pathogenic Th17 cells and production of IL-23p19 in spleen.

4.Discussions

Th17 has been considered to have a role in pulp-related inflammation and IL-17 produced from Th17 is considered pathogenic in osteonecrosis precipitation in pulp and periapical disease (Carlos, Anna Clara Aragão Matos, *et al*.). IL-23 which is upstream, of IL-17, is the cytokine responsible for the differentiation of the Th17 cells (Iwakura, Yoichiro, and Harumichi Ishigame.). As in the previous study by Song, Minju *et al.* where pulp and periapical inflammation were found to exacerbate MRONJ development, the first aim of the present study is to investigate the role of IL-23p19 in the precipitation of MRONJ lesions and if neutralizing serum IL-23p19 using monoclonal antibodies can ameliorate MRONJ lesion development in mice. For that, IL-23p19 neutralizing antibody was injected into the mice that were receiving high doses of Zoledronic acid. The first step was to assess the efficacy of both Zoledronic acid and the IL-23p19 neutralizing antibody in the presence of the other drug. We performed MicroCT and ELISA to validate Zoledronic acid and IL-23p19 neutralizing antibody respectively. The reduced incidence of the roughened borers and unfilled extraction socket in the Zol-treated groups validated the efficacy of Zoledronic acid in this model. Similarly, ELISA results confirmed that the serum IL-23p19 was completely neutralized upon treating with anti-

IL-23p19 antibody. Next step was to check the tissue changes that occurs on the IL-23p19 neutralization in pulp-exposed MRONJ lesions. The histological sections showed a markedly reduced incidence of empty lacunae and necrotic bone formation in the groups that received IL-23p19 neutralizing antibody which clearly indicates the role of IL-23p19 in the development of MRONJ lesions in the presence of preexisting periapical disease. Along with that it confirms that Il-23p19 neutralization can prevent the development of MRONJ lesions in pulp-exposure model in mice.

TRAP+ osteoclasts were found to be increased in the Zol-treated group in pulp exposure model, but there was no significant difference found in the osteoclast number at the extraction site when IL-23p19 was neutralized. The probable reason might be an early timepoint of sacrifice that was done to assess the utmost role of IL-23p19 in precipitating MRONJ under inflammatory condition. Vieira, Andreia Espindola, *et al.* found that the peak osteoclastic activity in the extraction socket is at Day 14. Also, we can conclude that IL-23p19 does not have a role in recruitment of osteoclasts at the necrotic bone area, although studies have shown that it has role in differentiation of osteoclast (Ju, Ji Hyeon, *et al.*, Bouchareychas, Laura, *et al*., Furuya, Hiroki, *et al.*). Similar to the observation made by Song, Minju *et al.* in pulp exposure model, the Zol-IgG group showed large and deeply stained multinucleated osteoclast nuclei which seem to be more detached from the sections. However, a closer examination revealed less detached and reduced size of the osteoclasts in the Zol-a-IL-23 group compared to the Zol-IgG group. Further investigation needs to be done to investigate the reason of such a morphological change in osteoclasts that occurs upon IL-23p19 neutralization in the Zol-treated pulp exposure-induced MRONJ lesions.

The next aim was to determine the local and systemic changes in the IL-23p19 localization and differentiation of the Th17 cells upon neutralizing IL-23p19 in serum. To assess the changes in the localization of IL-23p19 and T cells at the tissue level, IL-23p19 and

IL-23R were immunostained. Upon serum neutralization of IL-23p19, there was a significant reduction in the levels of IL-23p19 in tissue in the Zol-treated group. Moreover, the level of tissue IL-23p19 in the Zol-a-IL-23 group was found to be consistent with the Veh-IgG and Veh-a-IL-23 groups. Comparing this data with the histomorphometric data, suggests that tissue localization of IL-23p19 has a pathogenic role in the precipitation of necrotic bone in pulp-exposed MRONJ lesions. However, immunofluorescence for IL-23R, which is expressed by the memory T cells, did not show any significant difference between groups, although the IL-23R+ cells seem to be more lined up along the necrotic bone area. However, IL-23R is expressed by other cells like NK cells, monocytes, macrophages and dendritic cells (Tang, Chunlei, et al.). Hence, to be more specific for T cells, we need to do further staining to confirm the exact changes in the T cell localization in tissue.

To look more into the local changes in the IL-23/Th17 axis in the cervical lymph nodes, qRT-PCR was performed on these samples. The *IL-23p19* mRNA level in the cervical lymph nodes was found to be significantly reduced on neutralizing serum IL-23p19 in the Zol-treatment group, though it was not completely depleted, that might indicate some level of Th17 cell differentiation occurring even after neutralizing the serum IL-23p19. This was evident with no significant difference in the *IL-17A* mRNA levels between groups and a significant increase in the *RORγt* and *IL-6* mRNA levels in the cervical lymph nodes upon injecting the neutralizing IL-23p19 antibody in the Zol-treatment group. However, owing to our histomorphometric analysis which shows a significant reduction in the necrotic bone area and empty lacunae, we suggest that although some level of Th17 cell differentiation is taking place, the cells that are being differentiated might not be pathogenic. Th17 cells can be pathogenic or non-pathogenic and the type of Th17 cell that gets differentiated depends on the combination of cytokines associated. Yang, Tsan, *et al*. stated that the IL-6/IL-23/IL-1β combination cytokine is essential for pathogenic Th17 cell differentiation. Our mRNA level of *IL-1β* was found to be

significantly reduced in the neutralizing antibody injection group with Zol treatment, which suggests that the pathogenic Th17 cell differentiation is inhibited. Non-pathogenic Th17 has a regulatory role and studies proved that non-pathogenic Th17 produces IL-10 to maintain tissue homeostasis (Wu, Bing, and Yisong Wan.). Our *IL-10* and *Foxp3* mRNA levels have also shown to increase significantly in the Zol-a-IL-23 group suggesting differentiation of more regulatory immune cells. Hence at the local level, IL-23p19 level is reduced both at the tissue and cervical lymph nodes when IL-23p19 is neutralized in serum.in Zol-treated pulp exposed MRONJ lesions in mice.

In order to investigate the systemic changes caused by IL-23p19 neutralization in Zol-treated MRONJ lesions, ELISA was performed to check the levels of different inflammatory cytokine and qRT-PCR was performed to check the mRNA levels at the spleen. Neutralizing serum IL-23p19 resulted in the complete depletion of serum IL-17A and IL-17F which proves that IL-23p19 is upstream of IL-17A and IL-17F, and its role in the differentiation of pathogenic Th17 cells. Also, IL-12p70, another proinflammatory cytokine which induces Th1 cell differentiation (Ethuin, Frédéric, et al.), was also found to be significantly reduced upon IL-23p19 neutralization. Thus, IL-23p19 neutralization significantly reduced the inflammatory cytokine levels at the serum level. Moreover, spleen qRT-PCR for the Th17 cell markers did not show any significant difference in the levels of the mRNA for Th17 cell differentiation upon IL-23p19 neutralization, suggesting no changes occurring in the differentiation of the Th17 cells in the spleen. From these data, we can conclude that systemically, IL-23p19 neutralization is not causing any change in the spleen mRNA levels, although serum IL-23p19 and related inflammatory cytokines are reduced significantly upon neutralizing IL-23p19 in serum. Moreover, comparing the qRT-PCR data between the cervical lymph node and the spleen also brings to a conclusion that markers for the Th17 cells are induced at the local level only but not at the systemic level.

From the Immunofluorescence staining and qRT-PCR mRNA level for IL-23p19, it is evident that IL-23p19 was significantly increased upon Zol-IgG administration compared to the Veh-IgG at the tissue and at the cervical lymph node respectively. Hence at the local tissue level as well as in the local cervical lymph nodes, IL-23p19 is increased in the Zol-IgG administration groups when pulp was exposed prior to tooth extraction. But looking at the systemic level, IL-23p19 level was not changed in the Zol-IgG group compared to the Veh-IgG group which is evident from the serum ELISA for IL-23p19 and the spleen mRNA levels for markers for Th17 cell differentiation. These observations suggest that MRONJ is a local lesion and the changes in the IL-23/Th17 axis is occurring at the local tissue and cervical lymph node levels only.

5.Conclusion

From the present study, we can clearly demonstrate the role of IL-23p19 in precipitation of MRONJ lesions when a preexisting inflammatory condition is present. Also, we can conclude safely, that serum IL-23p19 neutralization can ameliorate MRONJ lesion development. However, it cannot fully diminish development of necrotic bone formation, which might be because of the other IL-23-independent inflammatory immune pathways or reduced osteoclastogenesis and osteoclastic differentiation due to IL-23p19 neutralization (Ju, Ji Hyeon*, et al*.), which needs to be explored more. Investigation needs to be done to study the morphological change in the osteoclast that occurs on neutralizing IL-23p19 in Zol-treated MRONJ lesions in mice. Further assessment needs to be done to check the phenotype of the tissue resident Th17 cells and examine the role of ‘pathogenic’ Th17 cells in MRONJ development. As part of future direction, we want to extend our research by assessing local and

systemic status of IL-23/Th17 axis using a pulp exposure model without performing tooth extraction at a time when inflammation reaches the highest level.

6.Figures and figure legends

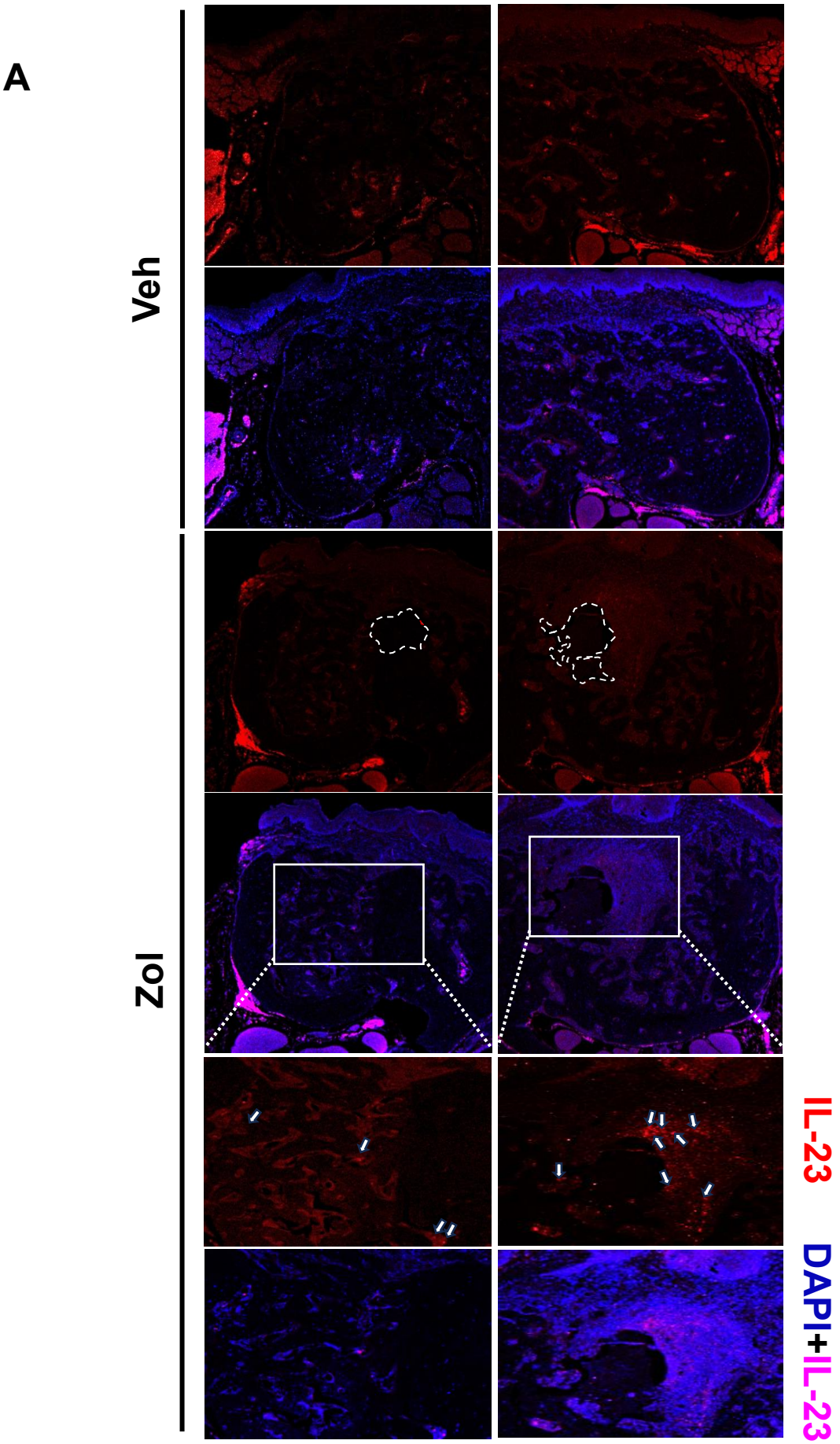

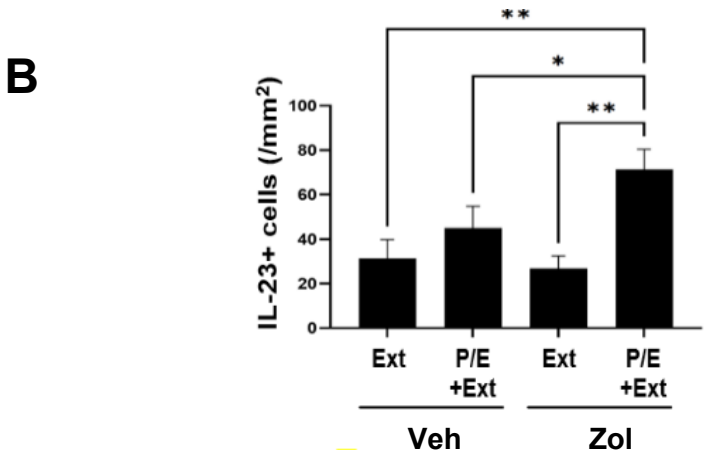

Figure 1- IL-23 is highly expressed around the necrotic bone area in pulp-exposed MRONJ lesions in mice. (A) Immunofluorescence-stained sections for IL-23p19. (B) Quantification of the number of IL-23p19+ signals. *p< 0.05, **p< 0.01.

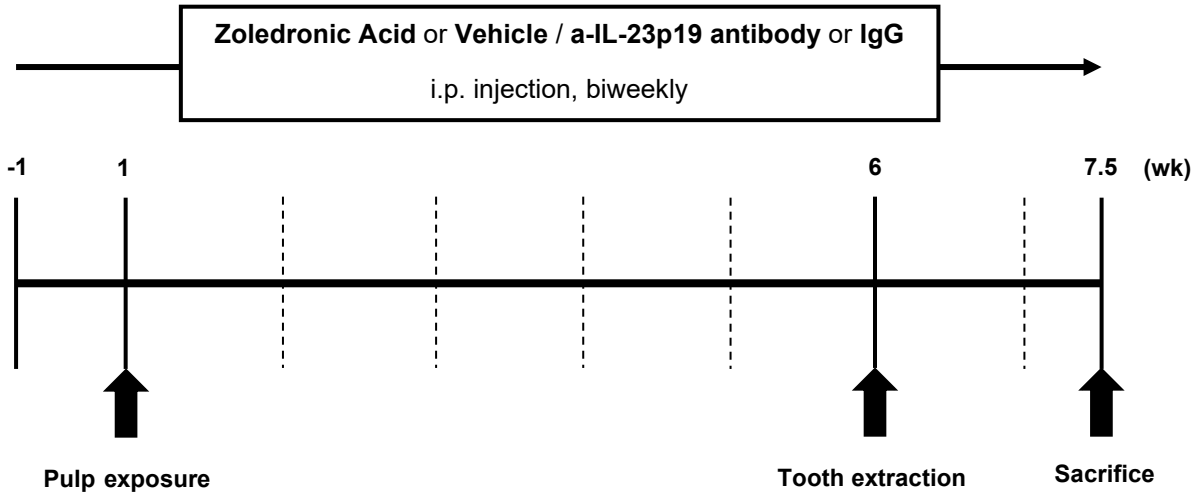

Figure 2- Study plan showing that pulp exposure was done on maxillary first molars one week following start of injection of Vehicle (Veh) or Zoledronic Acid (Zol) and IgG or a-IL-23p19 antibody. The teeth were extracted five weeks following the pulp exposure and mice were sacrificed ten days following tooth extraction.

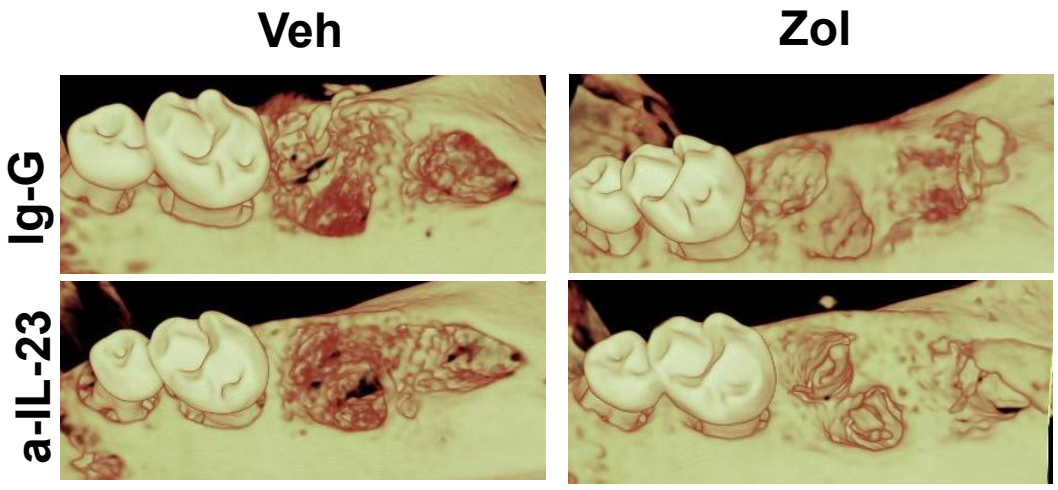

Figure 3- Validation of Zoledronic Acid treatment. µCT scanning was done on the maxillae 10 days following tooth extraction. 3-dimensional sections showing less incidence of roughened borders or unfilled socket upon Zoledronic Acid treatment.

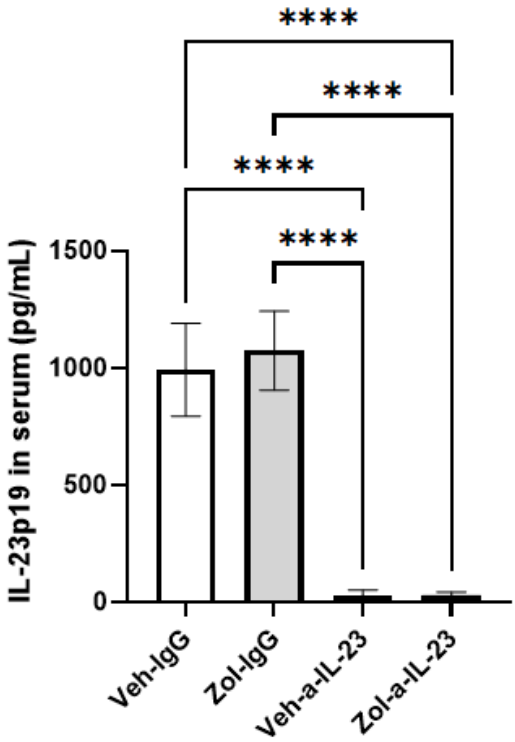

Figure 4- Validation of IL-23p19 neutralizing antibody treatment. Serum ELISA for IL-23p19 showed undetected levels of serum IL-23p19 upon IL-23p19 neutralizing antibody treatment. ****$p< 0.0001$.

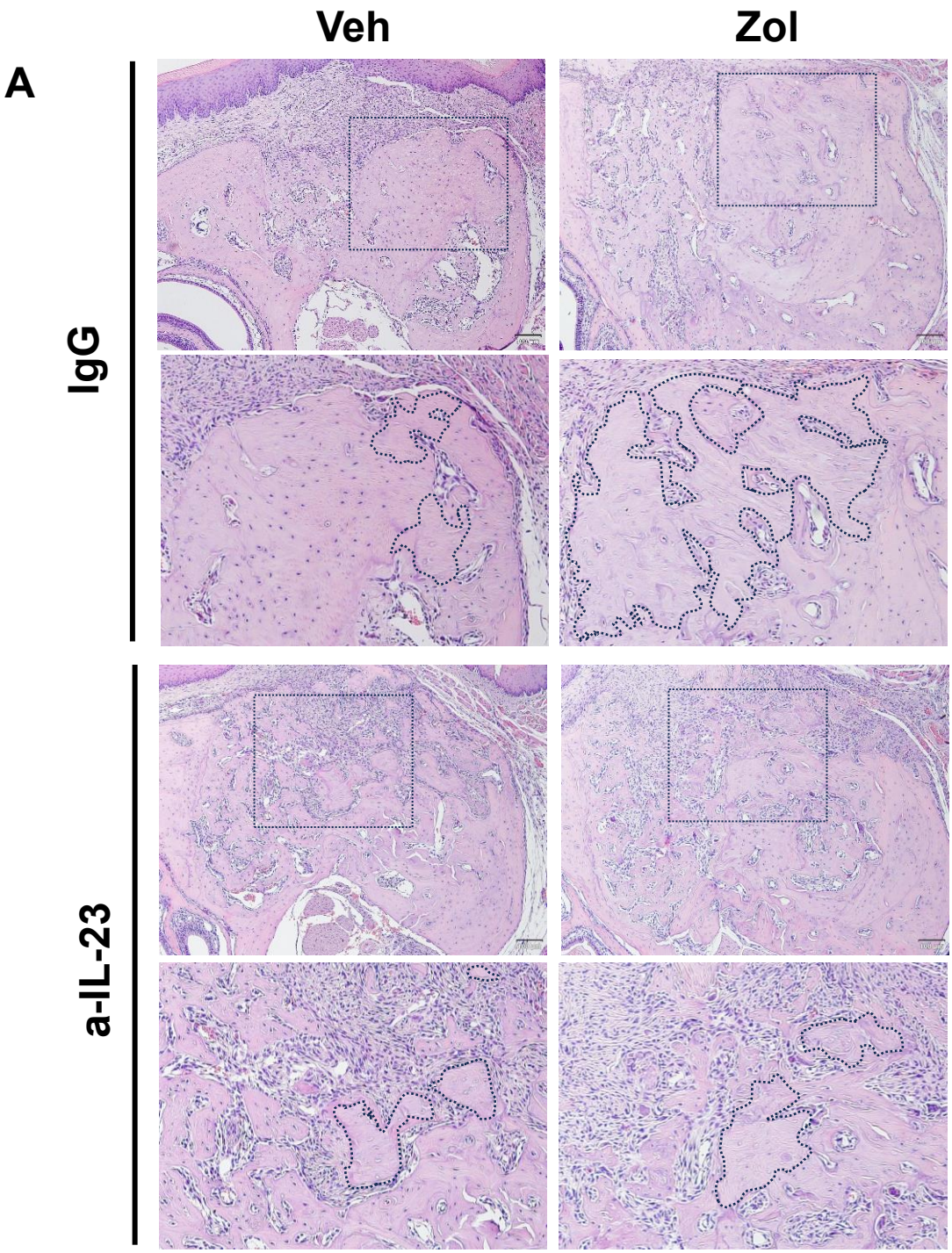
A
Veh
Zol
IgG
a-IL-23

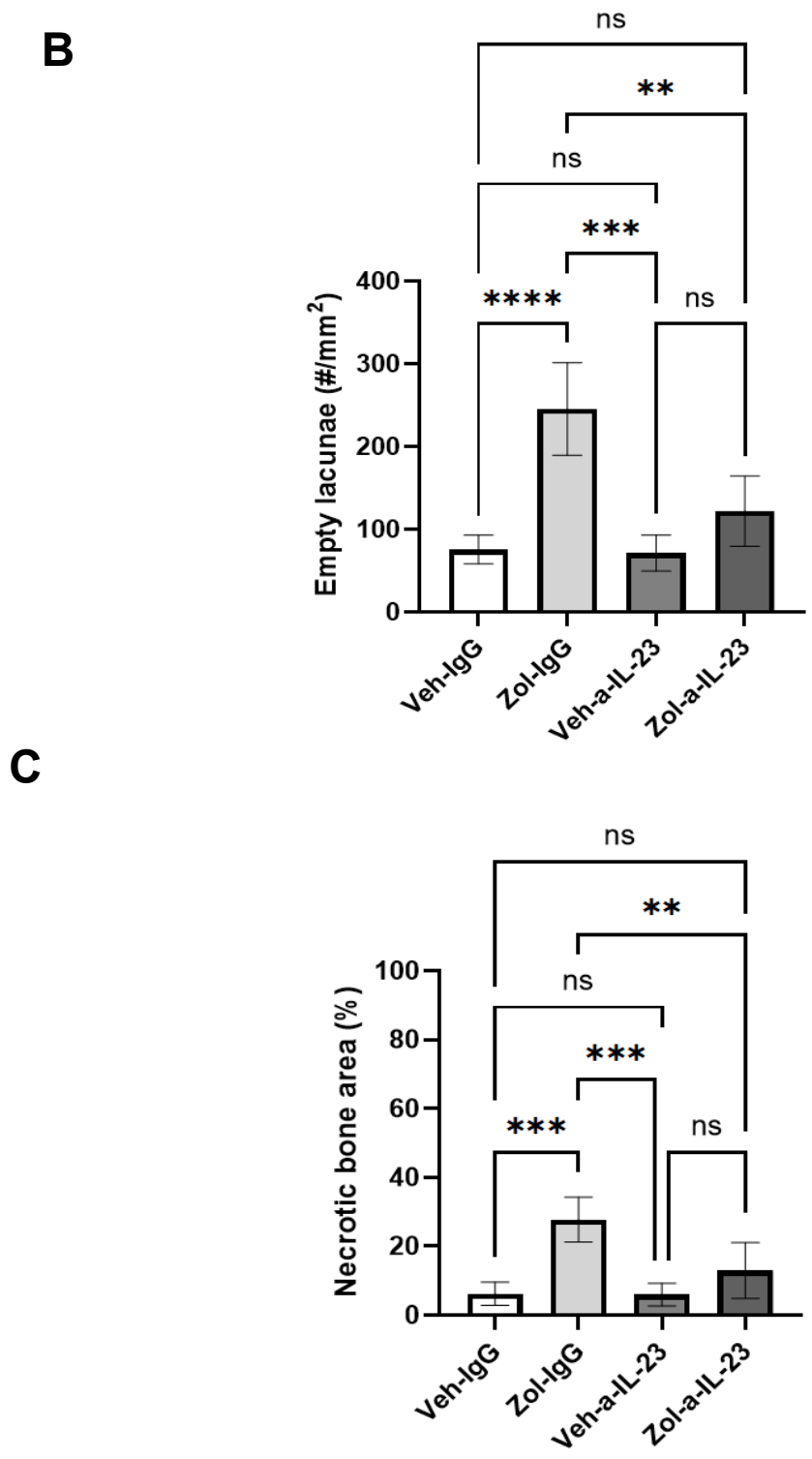

Figure 5- IL-23p19 neutralizing antibody ameliorates pulp-exposed MRONJ lesions in mice. (A) Hematoxylin and Eosin-stained sections of the site of extraction. Scale bar = 100 µm. Dotted lines indicate the necrotic bone area. Quantification of (B) empty lacunae, and (C) percentage of necrotic bone area per mm^2 bone area. $^{**}p< 0.01$, $^{***}p< 0.001$, $^{****}p< 0.0001$.

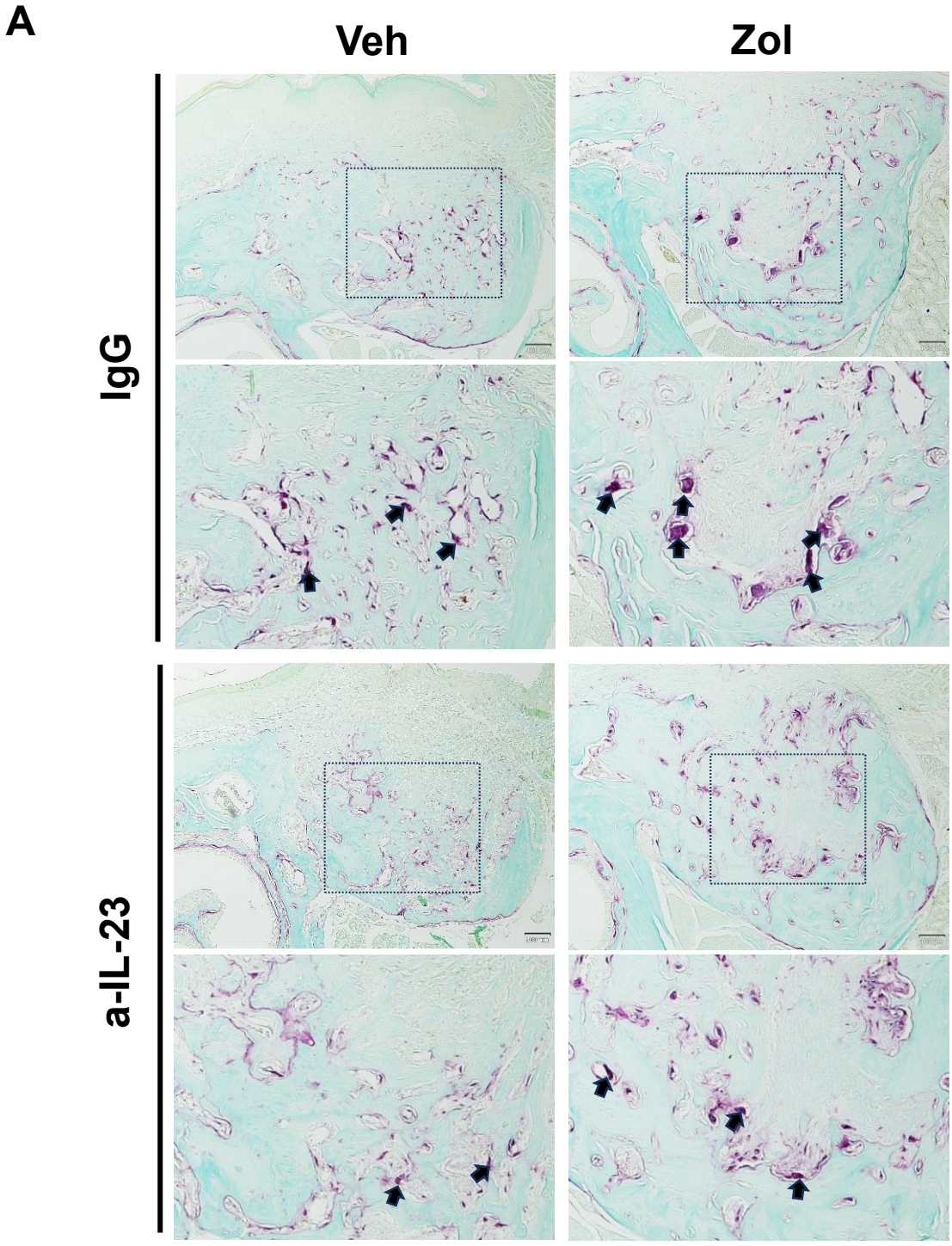
A
Veh
Zol
IgG
a-IL-23

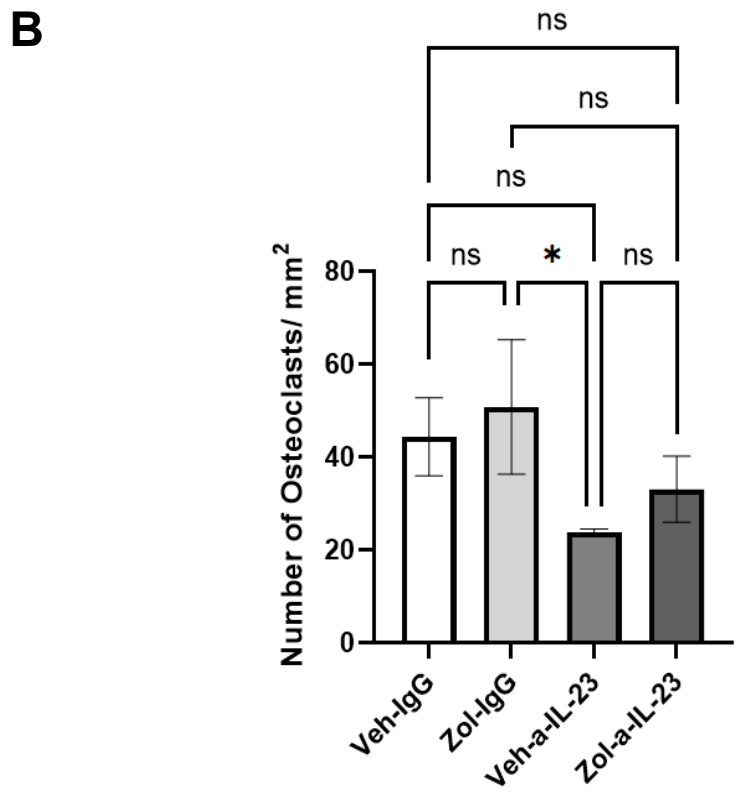

Figure 6- IL-23p19 neutralizing antibody does not affect osteoclast recruitment at the MRONJ lesion sites. (A) Tartrate-resistant acid phosphatase or TRAP-stained sections of the extraction socket. Scale bar = 100 μm. (B) Quantification of the number of TRAP+ osteoclasts per mm^2 bone area. *p< 0.05.

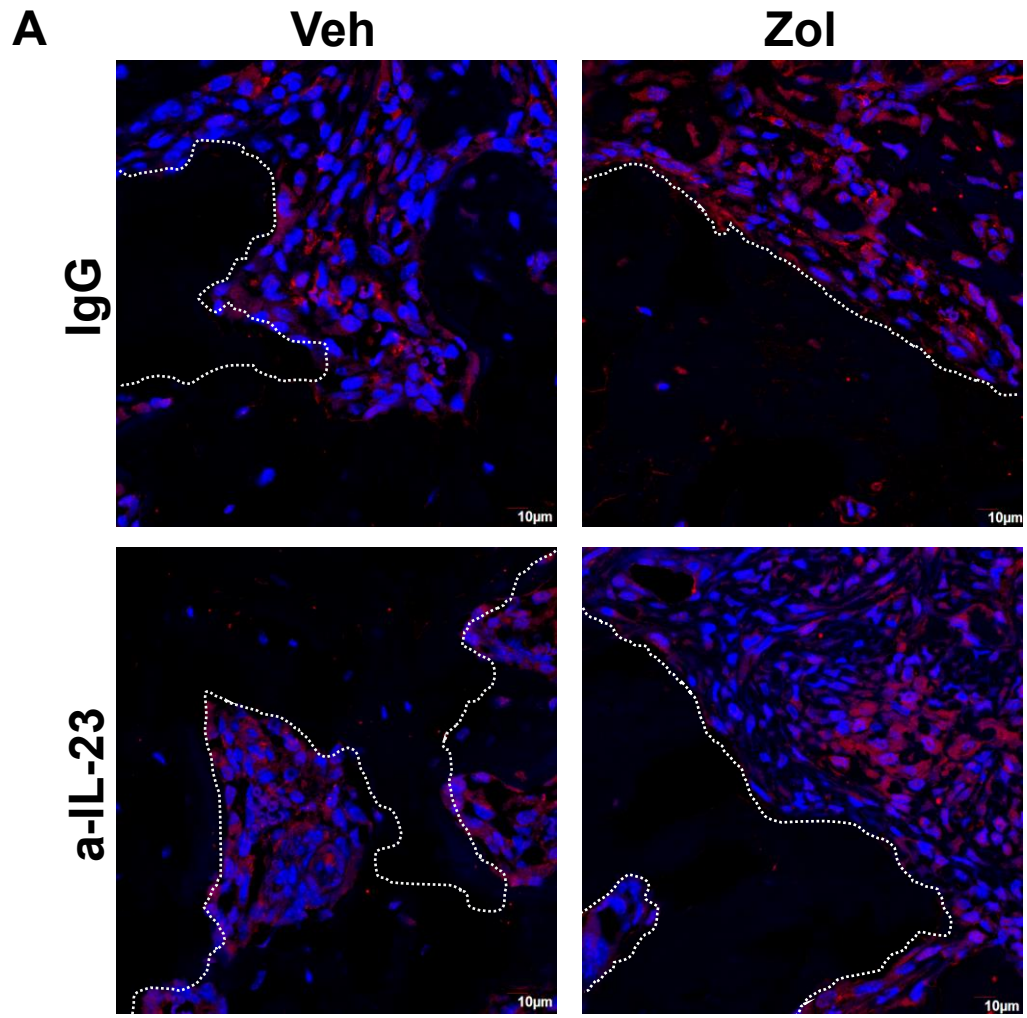
A
Veh
Zol
IgG
a-IL-23
10μm
10μm
10μm
10μm

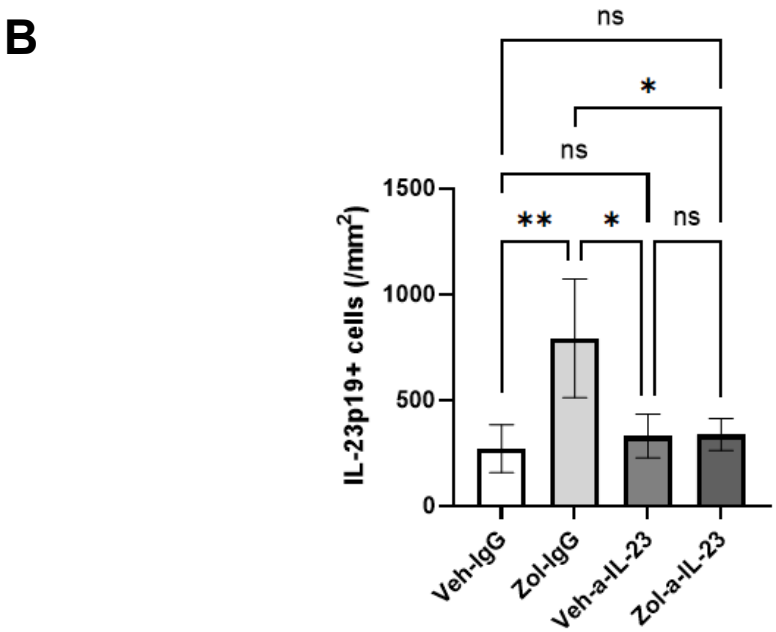
B
ns
*
ns
**
*
ns
1500
1000
500
0
IL-23p19+ cells (/mm2)
Veh-IgG
Zol-IgG
Veh-a-IL-23
Zol-a-IL-23

Figure 7- Serum neutralization of IL-23p19 leads to reduced IL-23p19 expression in the osteo-mucosal tissues. (A) Tissue sections stained for IL-23p19 antibodies. Scale bar = 10 µm. (B) Quantification of the IL-23p19 + cells around the necrotic bone area. *p< 0.05, **p< 0.01.

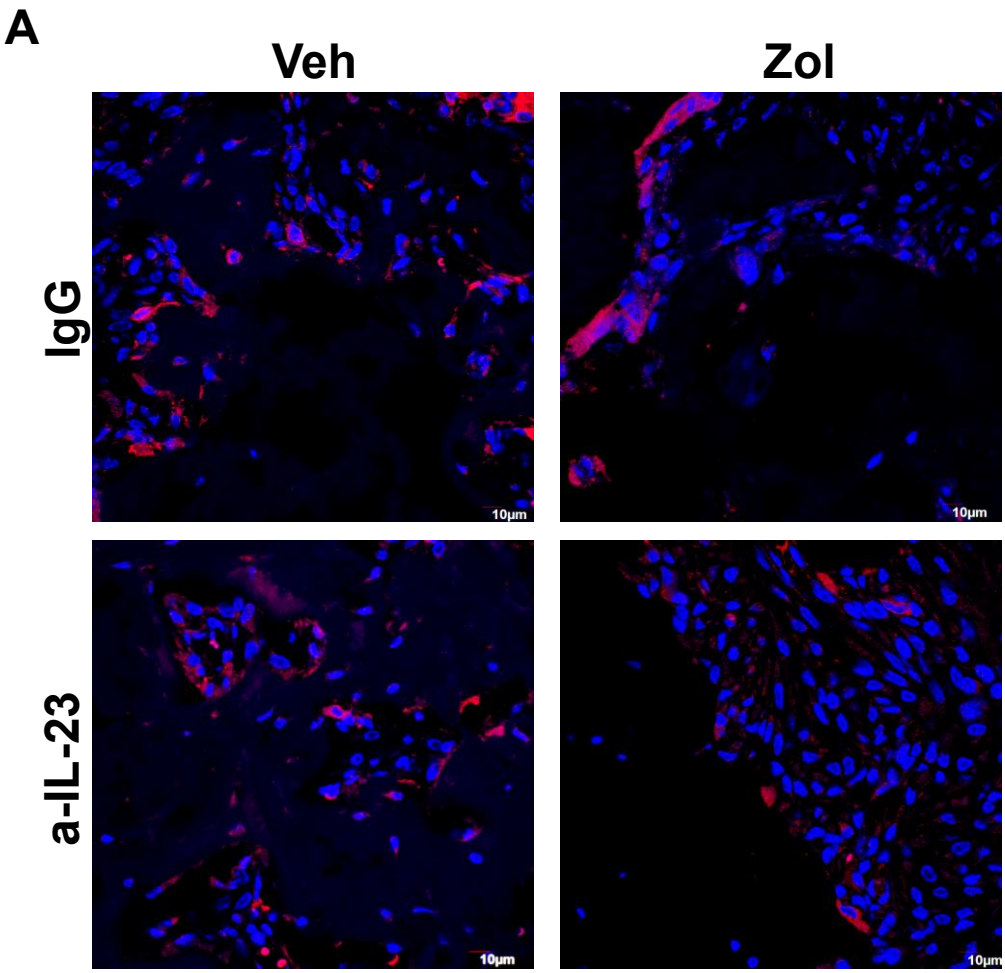

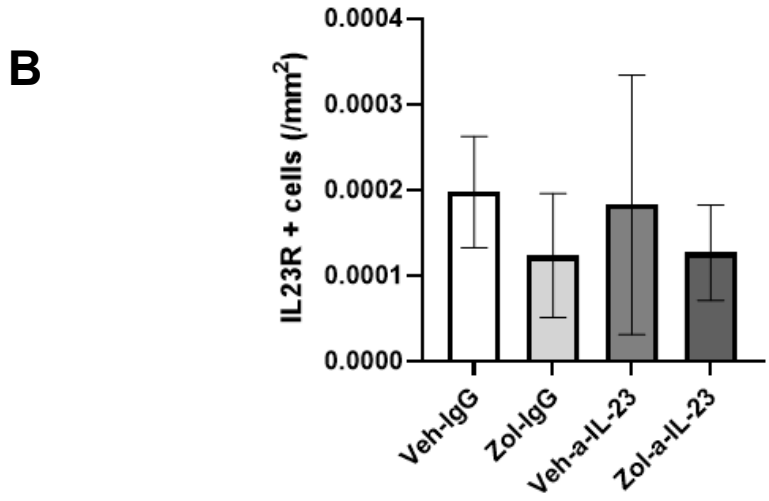

Figure 8- Serum neutralization of IL-23p19 leads to unaltered expression of IL-23R. (A) Tissue sections stained for IL-23R antibodies. Scale bar = 10 µm. (B) Quantification of the IL-23R + cells around the necrotic bone area.

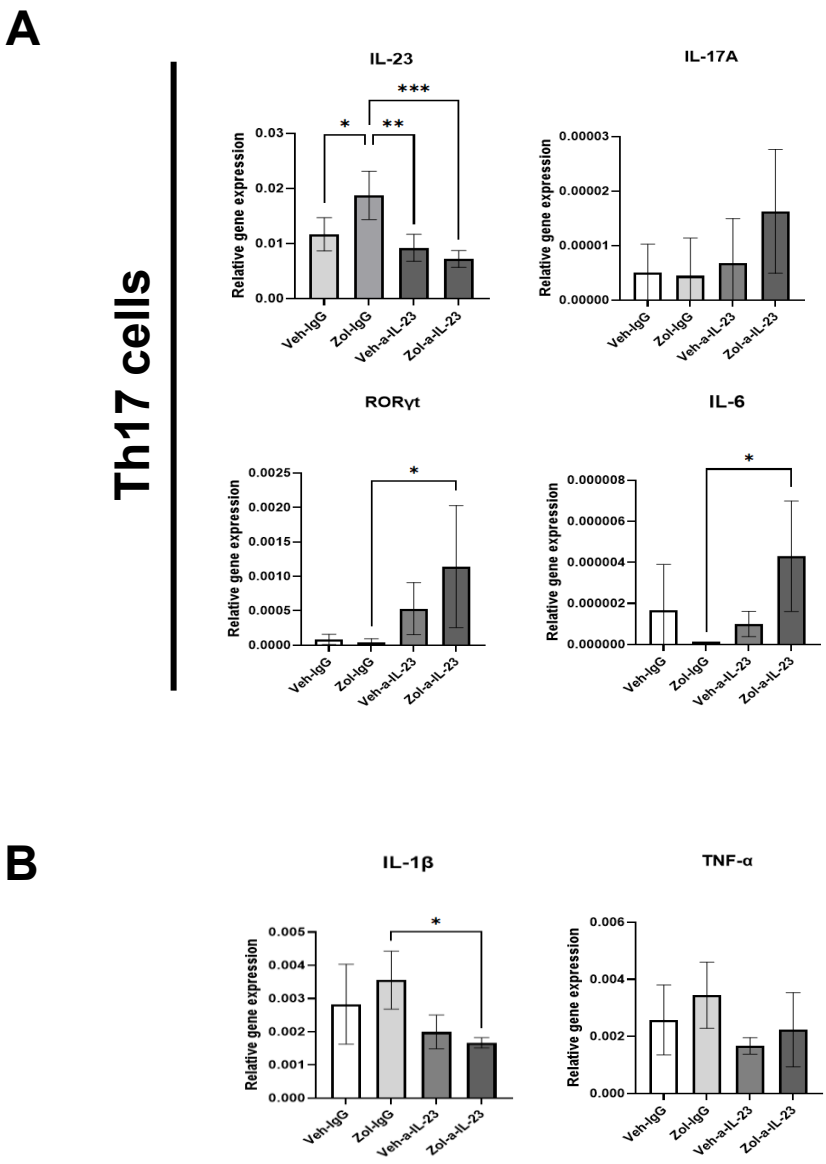

Figure 9- IL-23p19 neutralizing antibody causes reduced IL-23p19 synthesis in the cervical lymph nodes and reduced pathogenic Th17 cell differentiation. (A) qRT-PCR for *IL-23p19*, *IL-17A*, *RORγt,* and *IL-6* to determine Th17 cell differentiation. (B) qRT-PCR for *IL-1β* and *TNF-α*. *$p < 0.05$, **$p < 0.01$, ***$p < 0.001$.

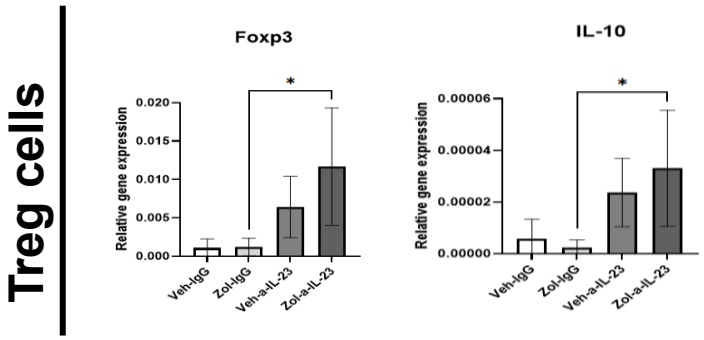

Figure 10- IL-23p19 neutralization causes increased Treg differentiation in the draining cervical lymph nodes. qRT-PCR for *Foxp3,* and *IL-10* to determine regulatory cell lineage differentiation. *$p< 0.05$.

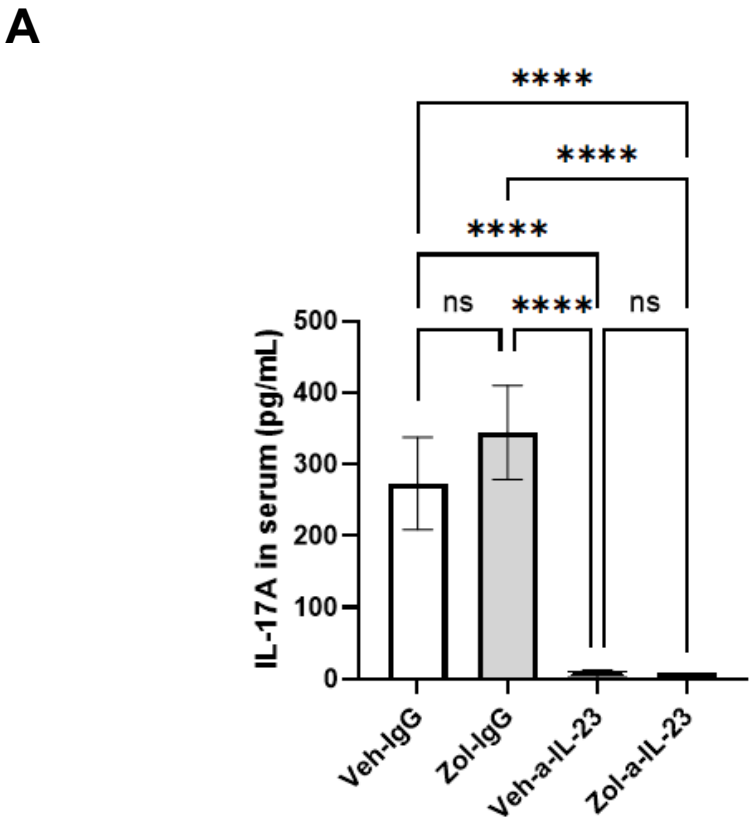

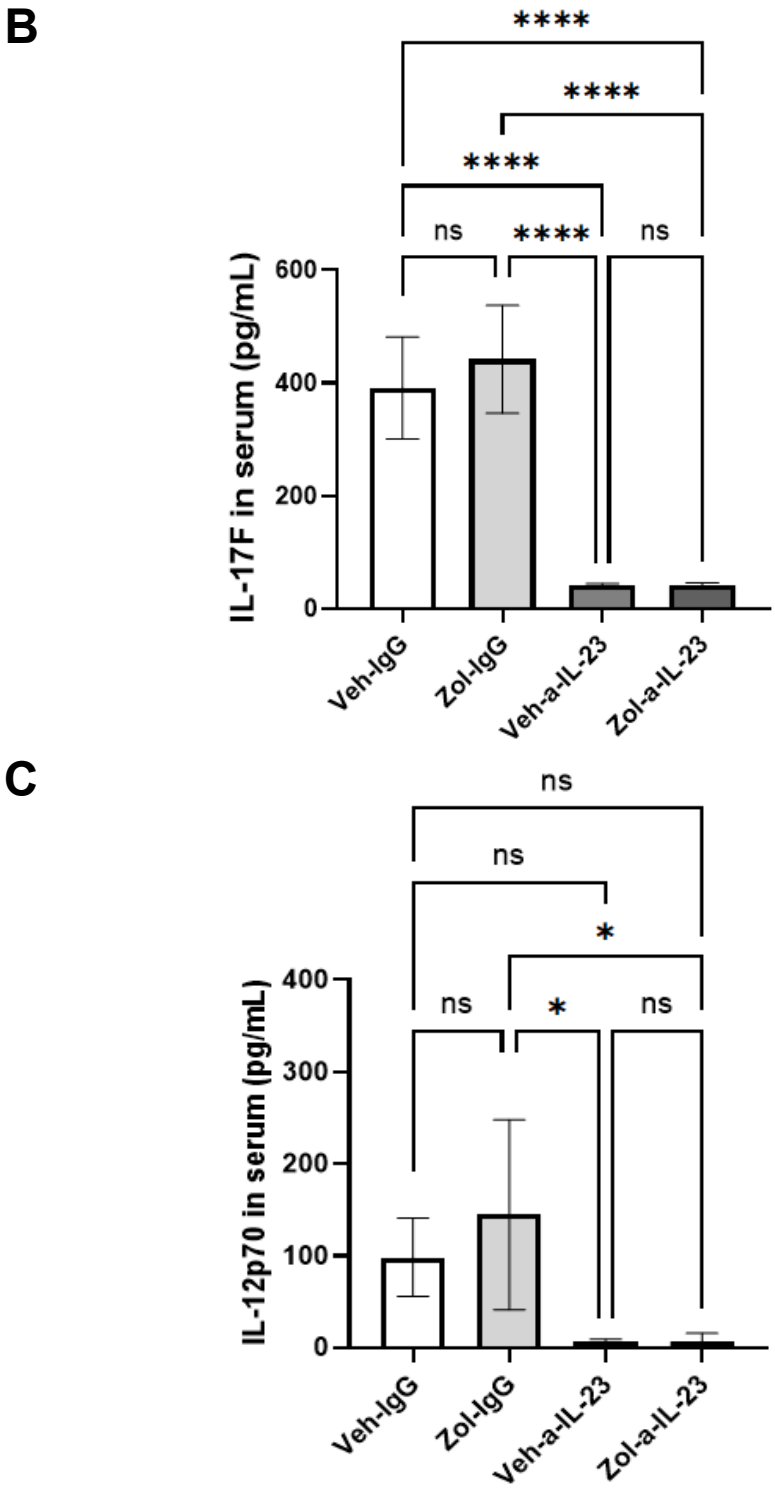

Figure 11- IL-23p19 neutralizing antibody leads to reduced inflammatory cytokine levels in serum. Serum ELISA for (A) IL-17A, (B) IL-17F, (C) IL-12p70 showing nearly undetected levels of the respective cytokines upon IL-23p19 neutralizing antibody treatment. *p< 0.05, ****p< 0.0001.

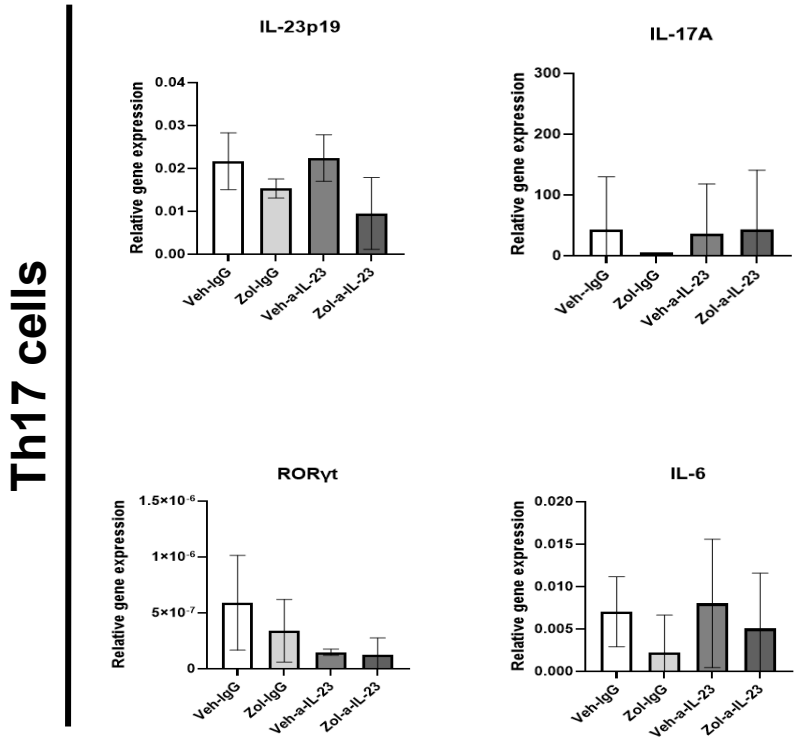

Figure 12- IL-23p19 neutralizing antibody has no effect on IL-23p19 and pathogenic Th17 cell differentiation in spleen. qRT-PCR for *IL-23p19*, *IL-17A*, *RORγt,* and *IL-6* to determine Th17 cell differentiation in spleen.

Gene	Sequence (5'-3')
mGAPDH	Forward: AGG TCG GTG TGA ACG GAT TTG Reverse: TGT AGA CCA TGTAGT TGA GGT CA
IL-23p19	Forward: TGT GCC CCG TAT CCA GTG T Reverse: CGG ATC CTT TGC AAG CAG AA
IL-17A	Forward: CAG GGA GAG CTT CAT CTG TGT Reverse: GCT GAG CTT TGA GGG ATG AT
RORγt	Forward: ACC TCC ACT GCC AGC TGT GTG CTG TC Reverse: CA TTT CTG CAC TTC TGC ATG TAG AC
IL-6	Forward: TAG TCC TTC CTA CCC CAA TTTCC Reverse: TTG GTC CTT AGC CAC TCC TTC
TNF-α	Forward: CCC TCA CAC TCA GAT CAT CTT CT Reverse: GCT ACG ACG TGG GCT ACA G
IL-1β	Forward: GCA ACT GTT CCT GAA CTC AAC T Reverse: ATC TTT TGG GGT CCG TCA ACT
Foxp3	Forward: AGA AGC TGG GAG CTA TGC AG Reverse: GCT ACG ATG CAG CAA GAG C
IL-10	Forward: TGG CCC AGA AAT CAA GGA GC Reverse: CAG CAG ACT CAA TAC ACA CT

Table 1- Oligonucleotide primer sets used for the detection of the cytokines and associated transcription factors for quantitative RT-PCR.

7.References

Song, Minju *et al.* “Preexisting Periapical Inflammatory Condition Exacerbates Tooth Extraction-induced Bisphosphonate-related Osteonecrosis of the Jaw Lesions in Mice.” *Journal of endodontics* vol. 42,11 (2016): 1641-1646. doi:10.1016/j.joen.2016.07.020.

Kim, Sol *et al.* "IL-36 induces bisphosphonate-related osteonecrosis of the jaw-like lesions in mice by inhibiting TGF-β-mediated collagen expression." *Journal of bone and mineral research* 32.2 (2017): 309-318.

Williams, Drake Winslow *et al.* “Long-Term Ligature-Induced Periodontitis Exacerbates Development of Bisphosphonate-Related Osteonecrosis of the Jaw in Mice.” *Journal of bone and mineral research: the official journal of the American Society for Bone and Mineral Research* vol. 37,7 (2022): 1400-1410. doi:10.1002/jbmr.4614.

Williams, Drake W *et al.* “Impaired bone resorption and woven bone formation are associated with development of osteonecrosis of the jaw-like lesions by bisphosphonate and anti-receptor activator of NF-κB ligand antibody in mice.” *The American journal of pathology* vol. 184,11 (2014): 3084-93. doi:10.1016/j.ajpath.2014.07.010.

Ruggiero, Salvatore L *et al.* “American Association of Oral and Maxillofacial Surgeons' Position Paper on Medication-Related Osteonecrosis of the Jaws-2022 Update.” *Journal of oral and maxillofacial surgery: official journal of the American Association of Oral and Maxillofacial Surgeons* vol. 80,5 (2022): 920-943. doi:10.1016/j.joms.2022.02.008.

Yazdi, Pouya Masroori, and Morten Schiodt. “Dentoalveolar trauma and minor trauma as precipitating factors for medication-related osteonecrosis of the jaw (ONJ): a retrospective study of 149 consecutive patients from the Copenhagen ONJ Cohort.” *Oral surgery, oral medicine, oral pathology and oral radiology* vol. 119,4 (2015): 416-22. doi:10.1016/j.oooo.2014.12.024.

Du, Wen, *et al.* "Indigenous Microbiota Protects Development of Medication-related Osteonecrosis Induced by Periapical Disease in Mice." *International Journal of Oral Science*, vol. 14, no. 1, 2022, pp. 1-8, https://doi.org/10.1038/s41368-022-00166-4.

Marx, Robert E *et al.* “Bisphosphonate-induced exposed bone (osteonecrosis/osteopetrosis) of the jaws: risk factors, recognition, prevention, and treatment.” *Journal of oral and maxillofacial surgery: official journal of the American Association of Oral and Maxillofacial Surgeons* vol. 63,11 (2005): 1567-75. doi:10.1016/j.joms.2005.07.010.

Baek, Hyeong-Jin *et al.* “Pulp and periapical disease as a risk factor for osteonecrosis of the jaw: a national cohort-based study in Korea.” *Journal of periodontal & implant science* vol. 54,2 (2024): 65-74. doi:10.5051/jpis.2300120006.

Hadaya, Danny *et al*. “Development of Medication-Related Osteonecrosis of the Jaw After Extraction of Teeth With Experimental Periapical Disease.” *Journal of oral and maxillofacial surgery: official journal of the American Association of Oral and Maxillofacial Surgeons* vol. 77,1 (2019): 71-86. doi:10.1016/j.joms.2018.08.010.

Zhu, Jinfang, and William E. Paul. "CD4 T cells: fates, functions, and faults." *Blood, The Journal of the American Society of Hematology* 112.5 (2008): 1557-1569.

Langrish, Claire L *et al.* “IL-23 drives a pathogenic T cell population that induces autoimmune inflammation.” *The Journal of experimental medicine* vol. 201,2 (2005): 233-40. doi:10.1084/jem.20041257.

Saravia, Jordy, *et al.* "Helper T Cell Differentiation." *Cellular & Molecular Immunology*, vol. 16, no. 7, 2019, pp. 634-643, https://doi.org/10.1038/s41423-019-0220-6.

Hoeppli, Romy E., *et al.* "The Environment of Regulatory T Cell Biology: Cytokines, Metabolites, and the Microbiome." *Frontiers in Immunology*, vol. 6, 2015, https://doi.org/10.3389/fimmu.2015.00061.

Moore KW, de Waal Malefyt R, Coffman RL, O'Garra A. Interleukin-10 and the interleukin-10 receptor. Annu Rev Immunol. 2001; 19:683-765. doi: 10.1146/annurev.immunol.19.1.683. PMID: 11244051.

Golubovskaya, Vita, and Lijun Wu. "Different Subsets of T Cells, Memory, Effector Functions, and CAR-T Immunotherapy." *Cancers*, vol. 8, no. 3, 2016, https://doi.org/10.3390/cancers8030036.

Tang, Chunlei, et al. "Interleukin-23: as a drug target for autoimmune inflammatory diseases." *Immunology* 135.2 (2012): 112-124.

Pastor-Fernández, Gloria, Isabel R. Mariblanca, and María N. Navarro. "Decoding IL-23 signaling cascade for new therapeutic opportunities." *Cell* 9.9 (2020): 2044.

Boniface, Katia, *et al.* "From Interleukin-23 to T-helper 17 Cells: Human T-helper Cell Differentiation Revisited." *Immunological Reviews*, vol. 226, 2008, p. 132, https://doi.org/10.1111/j.1600-065X.2008.00714.x.

Yang, Tsan, *et al.* "SENP2 Restrains the Generation of Pathogenic Th17 Cells in Mouse Models of Colitis." *Communications Biology*, vol. 6, no. 1, 2023, pp. 1-12, https://doi.org/10.1038/s42003-023-05009-4.

Zhang, Qunzhou *et al.* "IL-17-mediated M1/M2 macrophage alteration contributes to pathogenesis of bisphosphonate-related osteonecrosis of the jaws." *Clinical cancer research: an official journal of the American Association for Cancer Research* vol. 19,12 (2013): 3176-88. doi:10.1158/1078-0432.CCR-13-0042.

Carlos, Anna Clara Aragão Matos, *et al.* "Interleukin-17 plays a role in dental pulp inflammation mediated by zoledronic acid: a mechanism unrelated to the Th17 immune response?." *Journal of Applied Oral Science* 31 (2023): e20230230.

Liu, Mengyu, *et al.* "Interleukin-17 plays a role in pulp inflammation partly by WNT5A protein induction." *Archives of oral biology* 103 (2019): 33-39.

Hu, Y., *et al.* "Expression of a Cytokine, Interleukin-23, in Experimental Periapical Lesions." *International Endodontic Journal*, vol. 46, no. 10, 2013, pp. 896-903, https://doi.org/10.1111/iej.12077.

Ma, Nan *et al.* “Involvement of interleukin-23 induced by *Porphyromonas endodontalis* lipopolysaccharide in osteoclastogenesis.” *Molecular medicine reports* vol. 15,2 (2017): 559-566. doi:10.3892/mmr.2016.6041.

Coffelt, Seth B *et al.* “IL-17-producing γδ T cells and neutrophils conspire to promote breast cancer metastasis.” *Nature* vol. 522,7556 (2015): 345-348. doi:10.1038/nature14282.

de Molon, Rafael Scaf, *et al.* "OPG-Fc but not zoledronic acid discontinuation reverses osteonecrosis of the jaws (ONJ) in mice." *Journal of Bone and Mineral Research* 30.9 (2015): 1627-1640.

Wu, Bing, and Yisong Wan. "Molecular control of pathogenic Th17 cells in autoimmune diseases." *International immunopharmacology* 80 (2020): 106187.

Iwakura, Yoichiro, and Harumichi Ishigame. "The IL-23/IL-17 axis in inflammation." *The Journal of clinical investigation* 116.5 (2006): 1218-1222.

Vieira, Andreia Espindola, *et al.* "Intramembranous bone healing process subsequent to tooth extraction in mice: micro-computed tomography, histomorphometric and molecular characterization."*PloS one*10.5 (2015): e0128021.

Ju, Ji Hyeon, *et al.* "IL-23 induces receptor activator of NF-κB ligand expression on CD4+ T cells and promotes osteoclastogenesis in an autoimmune arthritis model." *The journal of immunology* 181.2 (2008): 1507-1518.

Bouchareychas, Laura, *et al.* "Critical Role of LTB4/BLT1 in IL-23–Induced Synovial Inflammation and Osteoclastogenesis via NF-κB."*The Journal of Immunology* 198.1 (2017): 452-460.

Furuya, Hiroki, *et al.* "Interleukin-23 Regulates Inflammatory Osteoclastogenesis via Activation of CLEC5A (+) Osteoclast Precursors."*Arthritis & Rheumatology* 75.8 (2023): 1477-1489.

Ethuin, Frédéric, et al. "Regulation of interleukin 12 p40 and p70 production by blood and alveolar phagocytes during severe sepsis. "*Laboratory investigation* 83.9 (2003): 1353-1360.